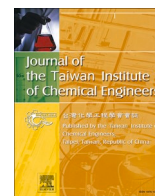




Since January 2020 Elsevier has created a COVID-19 resource centre with free information in English and Mandarin on the novel coronavirus COVID-19. The COVID-19 resource centre is hosted on Elsevier Connect, the company's public news and information website.

Elsevier hereby grants permission to make all its COVID-19-related research that is available on the COVID-19 resource centre - including this research content - immediately available in PubMed Central and other publicly funded repositories, such as the WHO COVID database with rights for unrestricted research re-use and analyses in any form or by any means with acknowledgement of the original source. These permissions are granted for free by Elsevier for as long as the COVID-19 resource centre remains active.



Energy and Environmental Science and Technology

Deciphering *Houttuynia cordata* extract as electron shuttles with anti-COVID-19 activity and its performance in microbial fuel cells

Chia-Kai Lin^a, Bor-Yann Chen^b, Jasmine U. Ting^c, Kristian Gil G. Rogio^d, Po-Wei Tsai^{e,*}, Yung-Chuan Liu^{a,*}^a Department of Chemical Engineering, National Chung Hsing University, Taichung 402, Taiwan^b Department of Chemical and Materials Engineering, National I-Lan University, I-Lan 260, Taiwan^c Department of Chemistry, College of Science, De La Salle University, Metro Manila 1004, Philippines^d School of Chemical, Biological, and Materials Engineering and Sciences, Mapúa University, Metro Manila 1002, Philippines^e Department of Medical Science Industries, College of Health Sciences, Chang Jung Christian University, Tainan 711, Taiwan

ARTICLE INFO

Keywords:

Electron shuttles (ESs)
Microbial fuel cells (MFCs)
Houttuynia cordata
Bioenergy extraction
Quercitrin
Flavonoids

ABSTRACT

Background: Traditional herbal medicines usually contain electron shuttle (ES)-like structures compounds which are potential candidates for antiviral compounds selection. *Houttuynia cordata* is applied as a biomaterial to decipher its potential applications in bioenergy extraction in microbial fuel cells (MFCs) and anti-COVID-19 via molecular docking evaluation.

Methods: *H. cordata* leaves extracts by water and 60% ethanol solvent were analyzed for total polyphenols, antioxidant activity, cyclic voltammetry (CV), and MFCs. The bioactive compounds of *H. cordata* leaves extracts were assayed via LC/MS analysis. Identification of the marker substances for potential antiviral activity using a molecular docking model was provided.

Significant findings: 60% ethanol extract exhibits the highest total polyphenols and antioxidant activity compared with water extracts. Bioenergy extraction in MFCs showed that 60% ethanol extracts could give 1.76-fold more power generation compared to the blank. Flavonoids and their sugar-to-glycan ratios increased after CV scanning and they are expected to be effective ES substances. Quercitrin, from the *H. cordata* extract that shares an ES-like structure, was found to exhibit strong binding affinities towards ACE2 and RdRp. This indicated the potential of *H. cordata* leaves as a promising antiviral herb.

1. Introduction

For thousands of years, Chinese medicinal herbs have been extensively used to treat diverse illnesses using their chemical composition and biological activity (e.g., antioxidant and anti-inflammatory) possibly due to combined synergy of compound formulae. Due to recent COVID-19 pandemics taken place over the globe, the variants of COVID-19 seemed not easy to be eliminated. Thus, it is of great importance to focus on searching for natural plants that can combat the virus and harness its rich phytochemical components in place of synthetic antioxidants due to their less toxic effects [1]. Recent studies reveal that COVID-19 treatment agents were abundant in ortho-dihydroxy substituents and flavonoids, which suggests that the herb may have electron shuttle (ES) capabilities and the ability to resist virus transmission [2]. As long as natural plants contain sufficient

polysaccharides and polyphenols, they will likely receive significant attention because such compounds have been referred to as “good antioxidants” [2]. To be specific, *H. cordata* was found to have the ability to persistently fight against COVID-19 [3,4]. These all directly suggest that such “good antioxidants” could be not such simple as stated. In fact, as Tsai et al. [5] pointed out, due to sustainable capabilities to effectively resist COVID-19, these “antioxidants” were found to be electron shuttles (ESs) with electrochemical catalysis. Hence, *H. cordata* will serve as a potential candidate for sources of natural ESs strongly related to power generation [6]. Thus, this study selects *H. cordata* as the main herb for analysis as its antiviral characteristics and ES capability can significantly stimulate organisms to catalytically accelerate the rate of redox reactions.

H. cordata (Family: *Cloveraceae*) is a perennial herb that grows in moist and shaded places. This plant is widely known among people of

* Corresponding authors.

E-mail addresses: powei@mail.cjcu.edu.tw (P.-W. Tsai), ycliu@dragon.nchu.edu.tw (Y.-C. Liu).<https://doi.org/10.1016/j.jtice.2023.104838>

Received 10 February 2023; Received in revised form 14 March 2023; Accepted 21 March 2023

Available online 3 April 2023

1876-1070/© 2023 Published by Elsevier B.V. on behalf of Taiwan Institute of Chemical Engineers.

different cultures in Japan, Korea, China and Northeast India for its medicinal properties. According to the practice of traditional herbal medicine, the plant has been often used to fight inflammation-related symptoms (e.g., pneumonia, severe acute respiratory syndrome, muscle sprains, and stomach ulcers). As a matter of fact, symptoms of oxidation and inflammation are usually taken place for most diseases. Many ancient documents of traditional Chinese medicine (TCM), Ayurveda, and Japanese traditional medicine also disclosed the anti-oxidative and inflammatory effects of *H. cordata* [7]. Among them, *H. cordata* was found to treat bronchial symptoms effectively. In terms of antiviral activity, *H. cordata* not only shows inhibitory activity against severe acute respiratory syndrome (SARS), but can also effectively fight against new coronary pneumonia COVID-19 [3,4,8]. In general, the chemical composition of *H. cordata* mainly falls into six categories, namely: volatile oils, flavonoids, alkaloids, fatty acids, sterols, and polyphenolic acids, as found from many studies [9–11]. The main active chemical components of *H. cordata* extract are identified as chlorogenic acid, rutin, hypericin, isoquercitrin, quercetin, afzelin, quercetin, catechol, caffeic acid, quinic acid, ferulic acid. Hence, to decipher the overall chemical reaction of *H. cordata*, LC/MS analysis was conducted herein to reveal whether the presence of these chemically active polyphenolic components could even exhibit strong ES potential.

Biomass-based energy is the most promising green renewable and ecologically compatible energy for sustainable development. To unveil such bio-compatible bioenergy content, microbial fuel cells (MFCs) harness the biocatalytic capabilities of living microorganisms, utilizing a wide range of organic matter to generate electrical current converting from chemical energy stored in chemical bonds. In this study, the MFCs contain three parts, i.e., anode, membrane and cathode. The anode is where the anaerobic oxidation occurs via the biofilm of *Shewanella* sp.—an electrochemically-active bacteria. Such electroactive bacteria mediate the process to release electrons (i.e., extracellular electron transfer) generated from oxidation of electron donors (e.g., sugars in the medium) through external circuit toward the cathode. These electrons are conserved in NADH fed into the quinol pool link to different inner membrane quinol oxidases transferred to outer membrane metal-reducing complex that either directly interacts on the surface of electrodes or indirect approach mediated by flavin electron shuttles [12]. The cathode contains a carbon electrode immersed in water that use dissolved oxygen as the electron acceptor or they are herein plain carbon electrodes in a ferricyanide solution. Using so-called electroactive bacteria, it is possible to generate bioelectricity by utilizing organic matter and degradable treated products (e.g., wastewater) [13,14]. Supplementation of exogenous ESs in MFCs can significantly "catalyze" the oxidation of organics and reduce the resistance to ET within the liquid phase and between solids and liquids, thereby considerably increasing bioenergy production. ESs act as "electrochemical catalysts" to enhance the rate of redox reactions and catalyze electron transport efficiency for abiotic and bioelectrochemical reactions, increasing power-generating capabilities of MFCs. Furthermore, it has been established that ESs are cost-effective and material-renewable which could potentially contribute to sustainable bioenergy extraction. Several studies have pointed out that chemical compounds bearing electron-shuttling structures (e.g., polyphenol oxides, aromatic compounds with *ortho*- and *para*-dihydroxy substituents) are capable of functioning as electrochemical catalysts that have reversible characteristics to stimulate redox reactions. However, for the *meta*-dihydroxy substituents, such promoting effect for electron-transporting characteristics could not be expressed due to the lack of resonance effect in the structure of the intermediate group [15–17]. Exogenous ESs are also known as redox mediators (RMs) which can be used as electro-active catalysts for energy extraction, reversibly promoting the electron transfer (ET) phenomenon for oxidation and reduction. Hence, the assistance through RMs provided the most energy-efficient and the least electron-resisting method for power generation in MFCs. Although supplementation with chemically synthesized ES (e.g., methylene blue, 2-aminophenol, or neutral

red) can significantly increase the rate of contaminant degradation, uses of synthetic chemicals are apparently not cost-effective or environment, ecology-friendly and even lead to concerns of secondary pollution after treatment. Therefore, adding natural sources of ESs to enhance the power-generating efficiency of MFCs is of great and immediate importance [16,18–20].

Meanwhile, Guo et al. [21] emphasized that neurological processes involve numerous redox processes comprising neurotransmitters (e.g., epinephrine and dopamine) which owns a structural moiety aiding effective electron-shuttling efficiency and considerably increasing bioelectricity-generating performance in MFCs. Due to the COVID-19 pandemics, recent studies pointed out that the electron-shuttling characteristics of chemical species in TCMs as RMs were associated with an effective antiviral activity following the "twofold index" of its amplification factor on power-generation in MFCs [22,23]. In fact, major compounds in *Rheum palmatum* L. (e.g., aloe-emodin, rhein, emodin, chrysophanol, and physcion) had significant MFC amplification factor and expressed antiviral effects on Flaviviridae viruses causing Dengue fever, Japanese encephalitis, and Hepatitis C [22]. Notably, a potential candidate for anti-COVID-19 treatment from *Coffea arabica*, which also satisfied the twofold MFC amplification factor, was found to be chlorogenic acid in molecular simulations [23]. The study revealed chlorogenic acid to have greater binding affinity to SARS-CoV-2 RdRp than remdesivir, resulting in stronger ligand-protein binding that terminates its viral transcription mechanisms. This pre-screening application of MFCs to natural products and synthetic chemicals for antiviral activity provides a novel platform in bio-electrochemistry leaning toward economically-feasible practices relevant to "bioenergy-steered" pharmacology for sustainable development.

In fact, herbal medicines were possible sources of natural ESs, since they have been used for disease treatment for thousands of years. Chen et al. [24] pointed out that naturally occurring ES source (e.g., medicinal herbs) are abundant in polyphenolic compounds which can be used as a potential bioresource to effectively stimulate the production of bioenergy in microbial fuel cells. In conclusion, this bioelectrochemical convertibility of natural polyphenolic antioxidants and ES will provide a sustainable alternative for renewable bioenergy applications. In particular, this feasibility study also emphasized that using indigenous bioenergy resources with green and sustainable significance of renewable energy utilization and recycling could achieve the goal of net-zero emission for circular economy.

This study therefore aims to investigate the effect of the different ratios of ethanol extracts on *H. cordata* leaves for the electrochemical activity via bioenergy generation. The phytochemical analysis for the quantification of the secondary metabolites in the form of total polyphenols and an evaluation of the antioxidant properties, and bioenergy production capability were also assessed. In addition, identification for marker substances using LC/MS for potential ESs compounds is carried out. The marker substances are further subjected to the antiviral activity tests using a molecular docking model for anti-COVID-19 treatment.

2. Materials and methods

2.1. Preparation of *H. cordata* leaves extracts

Fresh *H. cordata* was placed in the oven (50 °C) for one day, then grounded using blender into powder. Approximately 2.5 g of sample was placed in round flask with containing 50 mL of solvent and set up in a coiled condenser. Refluxed at 60 °C for 2 h, followed by suction filtration, and then concentrated using rotary evaporator. After filtration, the liquid was concentrated, and finally DI water was added to 50 mL quantitatively [24,25].

2.2. Cyclic voltametric (CV) assay

CV was then performed to compare the electrochemical properties of

different concentrations of *H. cordata* extracts. To test the electrochemical reversible stability of the samples, cyclic voltammetry scans were performed at a scan rate of 10 mV/s for 100 scan cycles using an electrochemical workstation (CHI-627A, CH Instruments Inc., USA). Initially, nitrogen gas was used to flush the herbal extract for 15 min. The working electrode, auxiliary electrode and reference electrode are glassy carbon electrode (0.07 cm²), platinum electrode (6.08 cm²) and Hg/Hg₂Cl₂ electrode filled with saturated KCl(aq), respectively. Glassy carbon electrodes (GCE, ID = 3 mm; model CHI-104, CH Instruments Inc., USA) were cleaned with 0.05 mm alumina polish before the study and then rinsed with 0.5 M H₂SO₄ and deionized water [17,24,26].

2.3. Total polyphenol contents

In this experiment, the total polyphenol content of the sample was determined by the Folin reagent method. Then the sample was filtered through a 0.22 µm filter sieve, 1 ml of the sieved sample was taken, and 2.5 ml of 0.2 mol/L (M) Folin phenol reagent (Sigma, USA) and 2 ml of 75 g/L Na₂CO₃ aqueous solution was added in sequence. The mixed solution was shaken with Vortex for 20 s to make the solution evenly mixed, the preparation process should be protected from light, placed in 45 °C incubator for 15 mins. after preparation, and finally Blue absorbance was measured at wavelength 765 nm by spectrophotometer (Genesys 20, Thermo, USA) [24,27].

2.4. DPPH free radical scavenging capacity

2,2-diphenyl-2-picrylhydrazine radical (DPPH, C₁₈H₁₂N₆O₅, Alfa Aesar) was used to evaluate antioxidant activity. DPPH scavenging capacity was measured by mixing 1 ml sample solution (prepared with 95% EtOH) with 2 ml of DPPH solution (0.0394 g DPPH/100 ml 95% EtOH). The mixture was allowed to stand in dark 30 min for reaction. Measure the absorbance at wavelength of 517 nm by spectrophotometer. The calculation formula of DPPH free radical scavenging ability is $(1 - (\text{Abs}_{\text{sample}} - \text{Abs}_{\text{blank}}) / \text{Abs}_{\text{control}}) \times 100\%$, where Abs_{sample} is the absorbance of 1 ml sample and 2 ml DPPH solution mixture; Abs_{blank} is the absorbance of 1 ml sample and 2 ml EtOH (95%) mixture; Abs_{control} is the absorbance of 1 ml EtOH (95%) and 2 ml DPPH solution mixture [24,28].

2.5. Power density

Power density was measured by using a self-designed dual-chamber (DC-MFC). Graphite rods (grade: IGS743; Central Carbon Co., Ltd) were used for anode and cathode. The cathodic and anodic compartments (volume 200 ml) were separated by a proton exchange membrane (DuPont™ Nafion® NR-212) with a contact area of approximately 200 ml for 4.52 cm² (inner diameter = 1.2 cm). The parameter anode is the actual working area of the graphite anode (16.49 m²). The MFC were operated at ambient temperature. Electroactive bacteria - *Shewanella sp.* (WLP72) was used for biopower generation in MFC. The strains were kept in -80 °C refrigerator. At the beginning of MFC, one tube of Eppendorf (containing 0.5 ml glycerol + 0.5 ml bacterial broth) is inoculated into a 500 ml Erlenmeyer flask containing 100 ml LB medium ((Difco™ LB Broth, Miller; Luria Bertani; composed of 10 g/L tryptone, 5 g/L yeast extract, and 10 g/L NaCl) as seed culture, then was incubated for 30 °C at 125 rpm incubator for 12 h. Then 1 ml of the seed culture was inoculated to the main culture in 500 ml Erlenmeyer flask containing 100 ml of LB medium and cultured for 30 °C at 125 rpm in an incubator shaker for 12 h. Before experimentation, the biomass OD_{600nm} was analyzed and ensured to reach about 1.8–2.0. Exactly 200 ml of the culture medium and 1 ml *H. cordata* extract were introduced into the anode tank. While the cathode cell was filled with electrolyte prepared from K₂HPO₄ (dipotassium hydrogen phosphate; SHOWA Co. Ltd.) and 6.38 g K₃Fe(CN)₆ (potassium ferricyanide; BAKER ANALYZED, A.C.S. Reagent) in 200 ml D.D. water. The culture medium without *H. cordata*

was used as reference and blank to determine effective power amplification after the introduction of the sample. The power and current density of the MFC are calculated using the following equations:

$$P_{\text{density}} = \frac{VMFC * IMFC}{A_{\text{anode}}} \quad (1)$$

$$I_{\text{density}} = \frac{IMFC}{A_{\text{anode}}} \quad (2)$$

where V_{MFC} and I_{MFC} can be assessed using linear sweep voltammetry by a program for electrochemical analysis [21,29].

2.6. LC/MS analysis

Liquid chromatography tandem mass spectrometer (Liquid Chromatography-Tandem Mass Spectrometer, LC/MS) was used. The model TSQ Altis produced by Thermo Scientific Company was a triple quadrupole mass spectrometer (Triple Quadrupole Mass Spectrometer). Ionization must be carried out first, and an appropriate ion source method should be selected according to the physical and chemical characteristics of the sample. In this experiment, electrospray ionization (ESI) was used to complete the scanning in the negative ion environment [6].

2.7. In-silico screening of the potential anti-COVID-19 activity of quercitrin

Proteins considered in this study were SARS-CoV-2 RdRp (PDB: 7BTF) and ACE-2 receptor (1R42). These proteins were obtained from PDB database (<https://www.rcsb.org/>) and processed in Biovia Discovery Studio 2021 and Autodock Tools 4.2 [30]. Before any analysis, these processed proteins were validated using different algorithms (Verify 3D and ERRAT) from UCLA Saves 6.0 (saves.mbi.ucla.edu) and Ramachandran plot (Anderson et al., 2005). To ensure the quality of the protein model used, Verify 3D (must be greater than or equals to 80%) that evaluates the 3D conformation of the protein based on its 1D sequence [31]. ERRAT (must be greater than or equals to 50%), was used to evaluate the distribution of non-bonded atomic interaction within the protein [31]. Lastly, the Ramachandran plot will show the percent of amino acid residues in the protein that was observed within the preferred and questionable region [32]. While, the sdf file format of the ligand used in this study (quercitrin, CID: 5280459) was obtained from PubChem (chem.ncbi.nlm.nih.gov). Then, OpenBabel [33] was used in converting the sdf file of the ligand to mol2 format for pharmacophore analysis (using PharmaGist) [34] and pdbqt format for docking analysis. Afterwards, AutoDock Vina [35] was used in this study for docking analysis on quercitrin and the six proteins. Comparing with the positive control, protein-ligand complex with promising binding affinity will undergo molecular dynamics simulation in CABS-Flex 2.0 [36]. All *in silico* analysis done in this study was conducted with a Window 11 computer system having AMD Ryzen 7 3700 U, Radeon Vega Mobile Gfx 2.30 GHz, and 8.00 GB RAM.

3. Results and discussion

3.1. The effect of ethanol concentration on cyclic voltammetry

To exhibit the optimal ratio of GRAS solvent to have maximal electro-activity for leading bioelectricity generation, cyclic voltammetry (CV) on electrochemical measure was implemented. In fact, the closed-loop area of the CV curve may be regarded as a probe to determine whether the electrochemical activity is reversibly stable [17]. Therefore, an electrochemical analysis via CV was also utilized to determine whether the electrochemical activity of the *H. cordata* extract exhibits ES characteristics. The area of the CV curve of the redox potential was used as an indicator of electrochemical activity. It is determined to assess

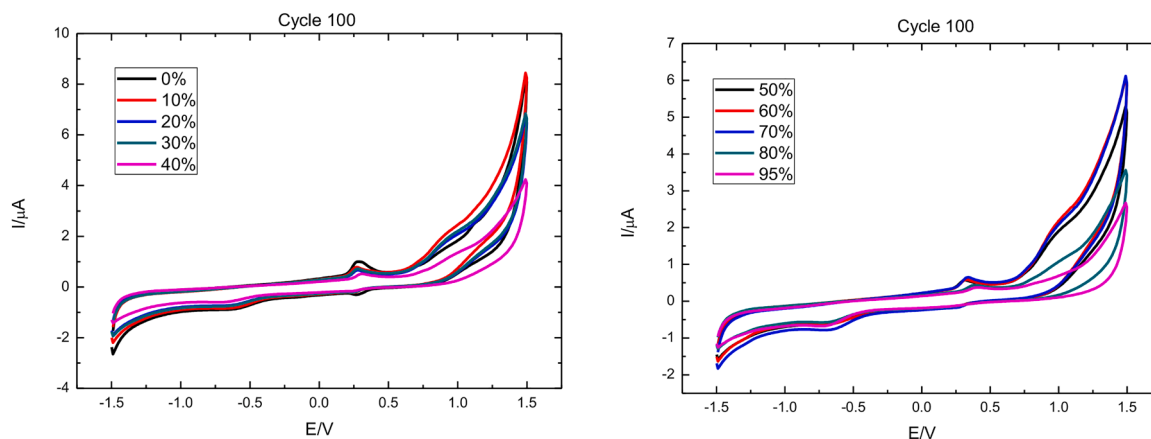


Fig. 1. Comparison of CV curves of different ethanol concentrations *H. cordata* extracts in 100 scans (a) ethanol concentration 0~40% (b) ethanol concentration 50~95%.

Table 1

Comparison upon different responding curves at various CV cycles of different ethanol concentration *H. cordata* extracts.

Ethanol Concentration	Cycle 1 (μW)	Cycle 10 (μW)	Cycle 50 (μW)	Cycle 100 (μW)	Decay ratio
95%	6.16	3.21	1.8	1.51	75.49%
80%	7.41	4.16	2.16	1.73	76.65%
70%	9.07	6.39	3.28	2.49	72.55%
60%	8.11	5.26	2.99	2.39	70.53%
50%	7.33	4.88	2.84	2.41	67.12%
40%	5.33	3.37	2.34	1.98	62.85%
30%	9.90	6.25	3.37	2.69	72.83%
20%	10.23	6.07	3.26	2.59	74.68%
10%	13.39	7.34	3.86	2.97	77.82%
0%	15.19	6.98	3.43	3.13	79.39%

^aSupplement is test of the *H. cordata* leaf extracts.

^bDecay ratio = $1 - (\text{Cycle } 100 / \text{Cycle } 1) \times 100\%$.

antioxidant capacity of the substance such that a higher area under the curve (AUC) indicates that the studied extract has a higher electrochemical potential to be expressed.

As shown in Fig. 1, the AUC of the different ethanol extracts after 100 CV scans, regardless of the ethanol concentration, possess similarity, and the shapes enclosed by the areas exhibit almost uniform. Fig. 1(b) showed an obvious second oxidation peak taken place in ethanol concentrations ranged from 50 to 70%. For quantitative evaluation, the area of each cycle curve was calculated (Table 1). As shown in Table 1, all AUC exhibited by the ethanol concentration of 50–70%, low-concentration ethanol, and pure water extraction is greater than 2 μW.

Significantly, water extraction remains an efficient condition with an area of 3.13 μW. According to Tsai et al. [5], the AUC value may not be regarded as the only screening factor, as the herbal extract may be not completely converted as appropriate electrochemical energy type(s) of biomass on the same basis. That is, the results may be influenced by the interference of various factors. In addition, further detailed analysis is inevitably required to elucidate the electrochemical characteristics of the extracts [17].

The stability and decay of the electrochemical activity of 60% ethanol *H. cordata* extract and 0% (pure water) extract were evaluated and analyzed. Under the cyclic voltammetry conditions, the scanning rate of 0.01 V/s, voltages ranged from -1.5 ~ +1.5 V and 100 serial scanning cycles, it was evaluated whether the extract can maintain good redox ability and sustainable energy during the long-term process of gaining and losing electrons. As Fig. 3 indicated, the closed-loop area is compared from the first to the 100th cycle (Table 1). It is found that the closed-loop area of the extract was consistent regardless of the concentration. In fact, from the first cycle to the 50th cycle, there is a significant downward trend which means that the redox-capable substances in the extract have electrochemically declined in the first 50 cycles of CV. Furthermore, the cycle area from the 50th to the 100th cycle is shown to be stabilized, suggesting that the electrochemical activity gradually decreases and converges to a stable level. Such transient dynamics of CV profiles would inevitably be deciphered in follow-up studies for conclusive remarks on catalytic potential.

As Fig. 2 revealed for comparison on the water extract and 60% ethanol extract, it is indicated that after 100 CV cycles, 0% ethanol extract changes more drastically than 60% ethanol extract. Therefore,

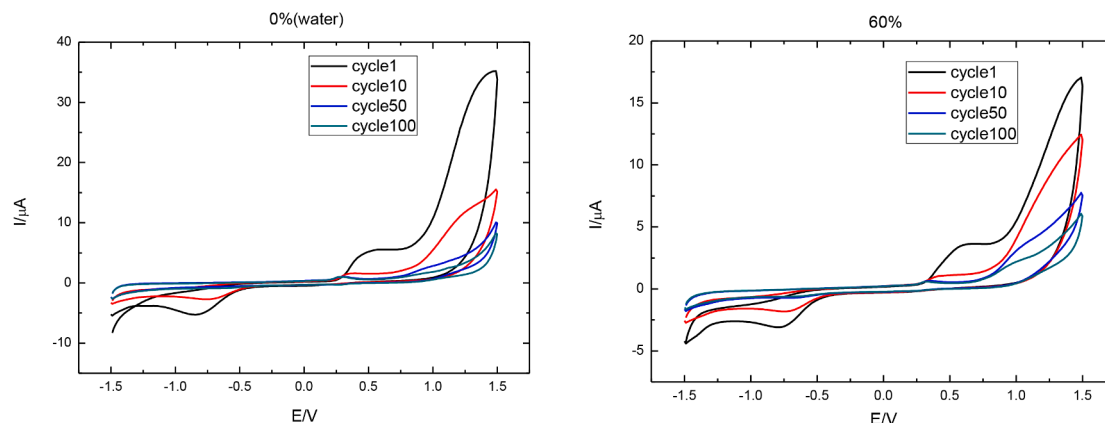


Fig. 2. CV curves of *H. cordata* water extract and 60% ethanol extract under different cycle.

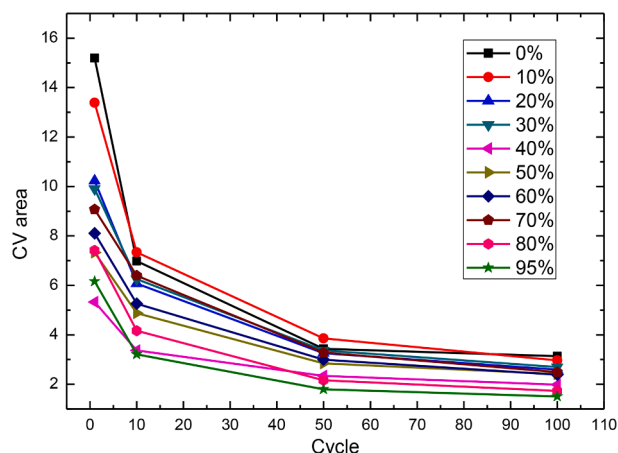


Fig. 3. The curve comparison of different CV cycle of different ethanol concentration *H. cordata* extracts (CV area unit in μW).

the trend for the decay rate seemed to be applicable to be an indicator. As a result, the decay rate of water extract was shown to be the highest, simply implying that the substances in water extract were relatively unstable than ethanol extract to be ESs. According to Guo et al. [21], antioxidant-rich chemicals can be gradually oxidized and/or attenuated after electrochemical treatment. However, for substances with strong electrochemistry and continuous reusability (i.e., substances with low decay rate), to achieve electrochemical stabilization, their potential will be reduced at first and then asymptotically stabilized. The remaining residual species would be very likely compositions with stable "electrochemical catalysis."

At the beginning of the scan, a rapid decline was exhibited, indicating that more substances in higher % ethanol extract cannot be electrochemically oxidized or reduced continuously (Fig. 3). There may be different amounts and diversity of impurities in water and ethanol. Specifically, after 50 scans, there is a gradual decay. According to prior studies, new peaks may be evolved after several cycles of cyclic voltammetry. It may be derived from the formation of polymer film on the glassy carbon electrode which obstructs the electrode that results in the CV AUC gradually decreasing [37,38]. This point is possibly consistent with the experimental results. The remaining persistent species strongly show that they have the electrochemically stable and reversibly properties of antioxidants. Evidently, substances with stable reductive and oxidative potential peaks (e.g., dihydroxy substituents chemicals) can significantly stimulate bioelectricity performance in MFCs [21]. That is, exposure to repeated electron donation and withdrawal processes, ESs can still stably maintain intact integrity of their chemical structures and electrochemical properties.

3.2. Ethanol concentration versus total polyphenol content

In the process of extracting phenolic compounds from plants, the properties of the extracted contents would vary due to the difference in the polarity of the solvents of extraction. According to "like dissolves like" principle, phenolic compounds favorable to such a solvent could thus be directly extracted. The quantitative analysis of the total polyphenol content of *H. cordata* was then tested by the Folin–Ciocalteu assay compared to unscanned CV results [39].

Relevant studies have pointed out that ethanol can effectively extract flavonoids and glycosides through the advantages of polarity in the extracting solution. Using organic solvents mixed with water helps form a medium polar solution, thereby improving the polyphenols extraction efficiency [40]. However, using water as a single solvent very possibly yields extracts with high levels of impurities (e.g., organic acids, sugars, soluble proteins) that may interfere with identifying and quantifying

Table 2

Polyphenol content of *H. cordata* extract at different concentrations.

Ethanol concentration	Before CV (mg GAE/g DW)	After CV (mg GAE/g DW)	Increase ratio
95%	27.44 \pm 2.12	27.67 \pm 0.86	0.83%
80%	38.33 \pm 0.55	40.33 \pm 0.24	4.96%
70%	40.17 \pm 0.16	43.05 \pm 0.63	6.69%
60%	49.50 \pm 0.16	56.22 \pm 1.18	11.95%
50%	48.83 \pm 0.16	51.44 \pm 0.24	5.07%
40%	42.72 \pm 0.16	44.50 \pm 1.25	4.00%
30%	34.89 \pm 0.39	39.38 \pm 1.57	11.40%
20%	31.00 \pm 0.24	32.61 \pm 0.47	4.94%
10%	24.28 \pm 0.16	31.72 \pm 0.16	23.46%
0%	22.56 \pm 0.08	22.61 \pm 0.63	0.22%

*GAE and DW represent as gallic acid equivalents and extract weight.

*Increase ratio = 1 - (Before CV / After CV).

phenolics [41]. In comparison with 60% ethanol and water extract, the water extract did contain the least amount of polyphenols while 60% ethanol with appropriate polarity yielded the most polyphenols. Ethanol effectively aids in the breakdown of the cell wall and enables the dissolution of phenolic compounds from the sample matrix. This is because most phenolic compounds are linked to lipophilic structures that may hinder it from extraction. Some polyphenolic compounds (e.g., flavonoids) are in the structure forms of glycosides. With the use of ethanol mixed with water as an extracting solvent, this helps form a medium polar solution, thereby improving the polyphenols extraction efficiency. Particularly, ethanol is a low polar solvent and water is a strong polar solvent so that can be mixed in any ratio. Therefore, after adding water to ethanol, the polarity of the composite solution increases continuously. That is, the proportion of more polar phenolic compounds obtained in the extract increased with water content. Another possible reason why the presence of some water would increase the efficiency could be due to the increased swelling of the plant material by water which increases the contact surface area between the plant substrate and the solution [42].

Chen et al. [17] pointed out that CV AUC gradually decreases and finally asymptotically stabilizes after several scan cycles. It is observed that this behavior exhibits a gradual electrochemical oxidation, indicating that they have the electrochemical properties of antioxidants. Thus, the antioxidant-rich chemicals could gradually be oxidized after electrochemical treatment. Whether electroactive species or chemicals can act as ES or antioxidants depends mainly on the reversible electrochemical properties of several serial CV scans under specific conditions. Furthermore, natural polyphenols could be irreversibly attenuated or reversibly remained via such repeated electrochemical oxidation and reduction would directly control the performance of bioenergy extraction in MFCs.

The analysis of the extract solution after cyclic voltammetric scanning was carried out to inspect whether the compounds were altered due to successive multiple redox reactions. As shown in Table 2, the polyphenol content of the extract evidently had change before and after CV processes. However, the maximum polyphenol content is still exhibited for the 60% ethanol extract regardless before or after CV scanning, suggesting that ethanol and water mixture have the most promising extraction efficiency in a specific ratio. The cyclic voltammetry measurements could increase the polyphenols level in the sample, which might be attributed to structural changes of chemical compounds in the extract, and improve the electrochemical properties for favorable bioelectricity stimulation for the electro-active bacteria.

3.3. Effect of ethanol concentration on power generation

As long as herbs rich in polyphenolic antioxidants can be efficiently converted into ES catalysts, it is highly suggested that this can effectively enhance the treatment efficacy of herbs to promote human health. For example, catechol and dopamine play critical bioenergetic roles in the

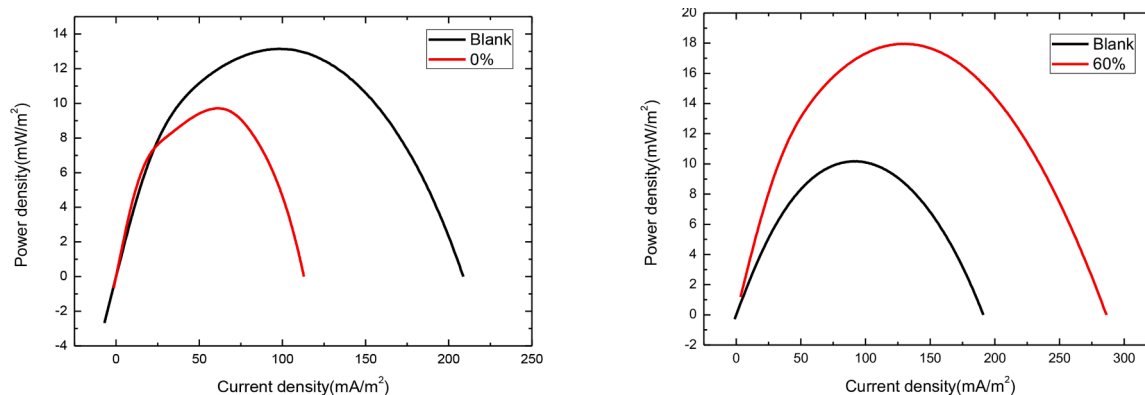


Fig. 4. Power density curves of *Shewanella* sp. WLP72 double chamber microbial fuel cell supplemented with (a) water extract; (b) 60% ethanol extract.

Table 3

Comparison of maximal power-generating capabilities of *Shewanella* sp. WLP72 inoculated double chamber microbial fuel cells (1000 mg / L).

EtOH Concentration	Max blank (mWm ⁻²)	Max sample (mWm ⁻²)	Amplification ratio of PD _{max}
95%	10.88	12.63	1.16
80%	10.56	12.88	1.22
70%	9.87	13.65	1.38
60%	10.18	17.96	1.76
50%	9.48	15.76	1.66
40%	13.27	14.83	1.12
30%	10.04	11.21	1.12
20%	10.85	11.24	1.04
10%	10.18	10.21	1.00
0%	13.14	9.71	0.74

*Max Blank: MFCs without supplement of *H. cordata* extract.

*Max Sample: MFCs supplemented with *H. cordata* extract.

*Ratio = Max Sample / Max Blank.

continued functioning of the body and brain related effects [21]. To validate the aforementioned analysis, *H. cordata* was used to evaluate bioelectricity-generating capability of MFCs and verify whether the residual chemical species could be ESs [18,24,43].

Moreover, studies [44,45] indicated that *Shewanella* could effectively catalyze simultaneous wastewater biodegradation and bioelectricity generation. This was due to encouraging electrical conductivity of bacterial nanowires produced by *Shewanella* strain. Through exogenous supplements of redox mediators, it can even improve forward the electron-transferring capability in MFCs. Furthermore, potassium ferri-cyanide in the electrolyte could be reduced through *Shewanella* sp. (WLP72). This process is required to release electrons by oxidizing organic matter (e.g., sugars) and increasing the overall reaction rate. Here, *H. cordata* extract was added to microbial fuel cells with *Shewanella* strain and different concentrations of ethanol extracts were inoculated (Fig. 4). The performance of supplemented *H. cordata* extract was compared as indicated in Table 3 and Fig. 4. The amplification of PD with respect to blank is ranking as follows: 60%(1.764) > 50%(1.662) > 70%(1.383) > 80%(1.22) > 40%(1.22) > 30%(1.117) > 20%(1.036) > 10%(1.003) > 0%(0.74).

The effect of 60% ethanol even more effectively increased the reaction rate in MFCs. Prior TPC analysis showed that 60% ethanol extract ranks the first place for the total polyphenols. On the contrary, the water extraction is less than the blank and thus exhibits no additive effect. That is, the polyphenol content contained in the water extracts was shown to obtain the lowest yield [17]. These variations seemed to suggest that there exists a correlation between the polyphenol content and ES. Very possibly due to electrochemical catalysis of ES species, the resultant extract could be considerably converted to nutrients with fewer carbon atoms in higher rates. Therefore, electro-active microorganisms could

Table 4

Comparison of power density curves of dual-tank microbial fuel cells inoculated with *Shewanella* sp. WLP72 in 60% ethanol and 0% ethanol extract of *H. cordata* before and after CV (1000 mg/L).

Supplement	PD ratio		Increase ratio
	Before CV	After CV	
60%	1.76	2.08	15%
0%	0.74	1.07	31%

* Ratio = Max Sample / Max Blank.

* Increase ratio = 1 - (Before CV / After CV).

effectively utilize the converted nutrient sources. Meanwhile, this electrochemical catalysis also effectively triggers the cellular metabolism of electron transport chain in the bacterial cells. This of course augmented bioelectricity production in MFCs due to significant reduction of electron transfer resistance among different phases (e.g., biofilm-to-electrode, broth medium-to-biofilm resistances). Such findings also confirm that the content of phenols affects electricity production efficiency due to different amount and chemical species of exogenous ESs. Following the previous analyses of total polyphenol content and CV profiles, the 60% ethanol extracts also exhibited the largest electrochemical potentials for redox mediations. Thus, 60% ethanol extract would be the most electrochemically promising for bioenergy extraction.

To verify whether the residual chemical species own electrochemical potential as ES or compounds exhibiting electrochemical attributes (e.g., electroreduction and/or oxidation potential peak(s)), *Shewanella* strain WLP72 was also used as a control to compare the changes of water and ethanol extracts after 100 CV scans. Apparently, the results indicated that both extracts showed significant increases in power amplification after CV scan (Table 4). In terms of the increased ratio from the before CV to after CV, the increase percent ratio in the water extract was shown to be larger. It can thus be suggested that substances in the extract change, wherein new substance(s) were formed to provide electrochemically favorable stimulation to bioelectricity generation of *Shewanella*. Aware that this stimulation should augment the rate of power generation, but total contents of bioenergy to be released still remained identical. Electrochemical “catalysts” would not involve in reactions and total amount will be fixed before and after reactions. However, as Table 4 and Fig. 5 revealed, the power generation amplification due to water extraction was obviously not ideal. The study by Huang et al. [6] pointed out that the water extraction substances had inhibited or considerable biotoxicity potency; thus, ca. 26% production of electricity was reduced. However, after CV scanning, it was found to significantly reduce biotoxicity and effectively increase (31%) the electricity production. Due to considerable reduction of electron transfer resistance, it is suspected that the biotoxicity potency of the extract after CV

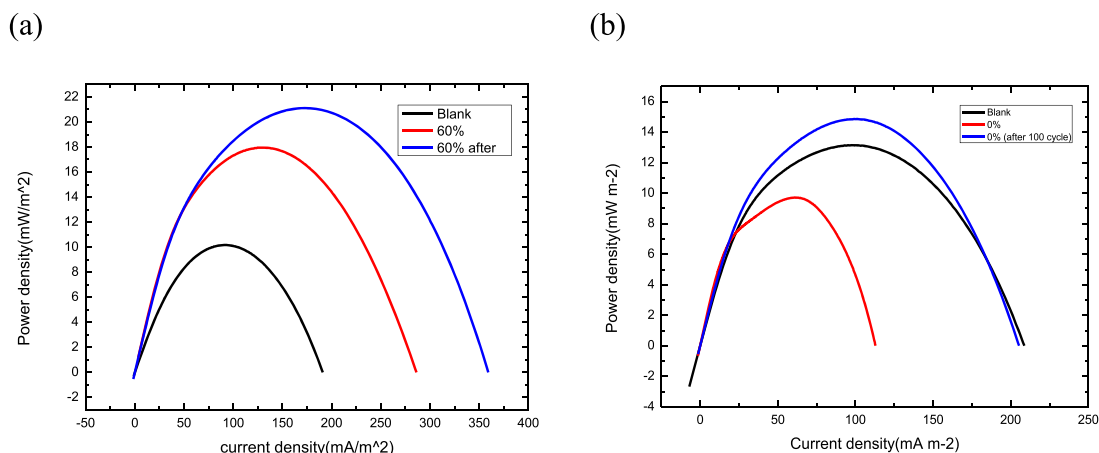


Fig. 5. The power-generating curve of the dual-chamber microbial fuel cell inoculated with *Shewanella* sp. WLP72, filled with (a) *H. cordata* 60% ethanol and 60% ethanol extract after CV (b) *H. cordata* 0% ethanol and 0% ethanol extract after CV treatment.

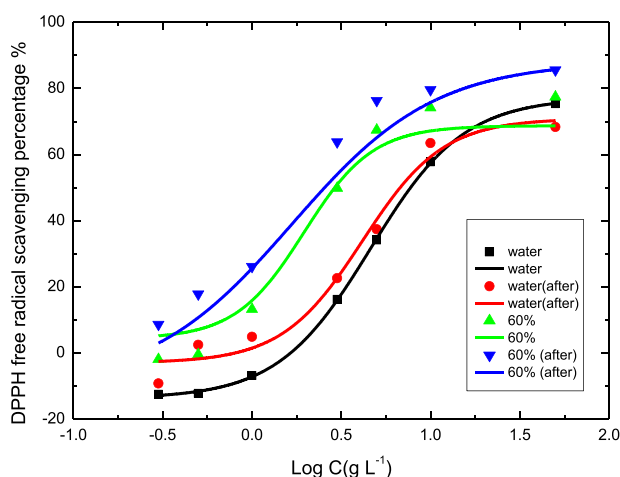


Fig. 6. Comparison of dose-response curve comparison of DPPH radical scavenging activity of *H. cordata* in 60% ethanol and water extraction before and after cyclic voltammetry scanning.

treatment was attenuated or the inhibitory substances were significantly reduced. Thus, this would increase bioelectric power density in MFCs. That is, the *H. cordata* residues after CV treatment could still be used as a sustainable synergic stimulus with efficacy for biomass energy extraction [6].

As Tsai et al. [5] pointed out, if the PD can be amplified more than 2-fold, herbal extracts may possess antiviral activity, especially for herbs containing *ortho*-positioned dihydroxyl compounds, flavonoids which are crucial compositions to stimulate conversion of bioenergy into electric energy. In fact, glucose can be effectively converted into electrical energy and the continuous existence of sugar in the extract is beneficial to “electrochemical catalysis” and/or electro-oxidation of flavonoids [46,47]. To sum up, *H. cordata* ethanol extraction after CV scanning could accumulate more amounts of effective ESs with low toxicity to augment power generation efficiency. Supplement of CV-treated *H. cordata* extract to MFCs would significantly enhance power-generating capacity of MFCs, as CV process altered the substance to be more favorable to bioelectricity stimulation. Of course, chemical compositions before and after CV, LC/MS was thus applied to characterize the compounds present as shown afterwards.

3.4. DPPH free radical scavenging analysis

As antioxidants, ESs were also electrochemically active species, free

Table 5

Comparison of effective concentrations at 50% response (EC₅₀) of the dose-response curve of DPPH radical scavenging activity of *H. cordata* in 60% ethanol and water extraction before and after CV (unit: g/L).

		0%	60%
EC ₅₀	before CV	11.775	6.452
		(y = 1.2959x + 3.612)	(y = 1.1501x + 4.0687)
	after CV	11.913	3.907
		(y = 1.3532x + 3.5439)	(y = 1.3275x + 4.2142)

*Supplement is tested with the extracts of *H. cordata* leaves.

radical scavenging ability and electron-shuttling activity of polyphenol-rich plant species (e.g., herbs and *Camellia* tea extracts) are likely to be electrochemically related. That is, the DPPH free radical scavenging activity should be equally related to the electrochemically redox-mediated capacity of ES production in MFCs. The DPPH free radicals scavenging is commonly used to exhibit the potentials of antioxidants. As shown in Fig. 6, the antioxidant activity ranking of *H. cordata* at different ethanol extraction concentrations based on DPPH free radical scavenging ability is shown. However, to clarify the elucidation of the figure; effective concentration (EC_x) using the Probit model conversion equation was adopted for quantitative comparison.

$$Y = A + B \log Z \quad (3.1)$$

Y is the unit of Probit, A and B are the intercept and slope of the dose-response curve, Z is the dose concentration of DPPH free radical scavenger (unit: g/L) and

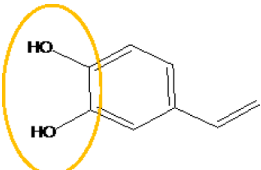
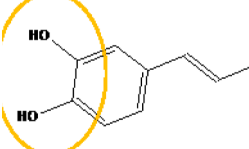
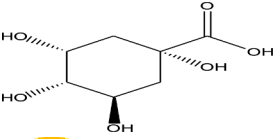
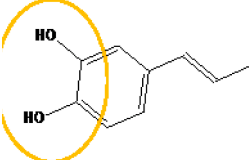
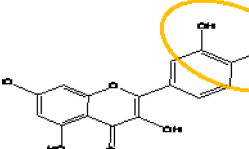
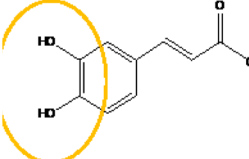
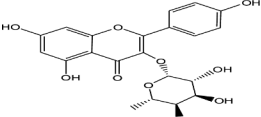
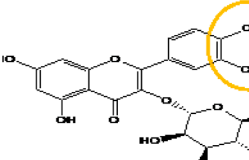
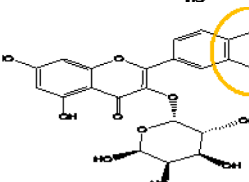
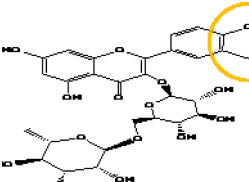
$$P = 0.5 [1 + \operatorname{erf} [(Y - 5) \sqrt{2}]] \quad (3.2)$$

P is the scavenging rate (unit: %) of the test substance to DPPH free radicals, and erf is the error function.

After successive calculations, the DPPH free radical scavenging and antioxidant capacity of the different ethanol extract using EC_x for comparative evaluation of various test samples with different antioxidant potencies (Table 5). EC₀ and EC₁₀₀ are the maximum concentration with detectable antioxidant response and the lowest concentration with 100% response, respectively. Based on dose-response assessments of EC₀, EC₂₀, and EC₅₀, the antioxidant capacity of the test substance can be estimated. Specifically, EC₅₀ is the concentration that exhibits 50% of standard activity relative to the reference DPPH free radical scavenging rate such that the antioxidant activity induced between concentrations of test substances between threshold (EC₀) and maximum (EC₁₀₀) [6,24,48]. From Table 5, the 60% ethanol extract, the extract after cyclic voltammetry scan is still larger than the unscanned extract, the EC₅₀ ranking as follows: 60% ethanol extract after CV > 60% stock solution.

Table 6

List of LC/MS results inferred components, and structural tags encircling ortho-dihydroxyl substituents [8–10].

Compound	Molecular Weight (g/mol)	Chemical Structure	0% EtOH	0% EtOH (after CV)	60% EtOH	60% EtOH (after CV)
1 4-Vinylcatechol	136.148		++	-	+	-
2 Caffeic acid	180.16		++	-	++	+
3 Quinic acid	192.17		++++	+	++++	++++
4 Ferulic acid	194		++	-	-	-
5 Quercetin	302.23		+	+	+	+
6 Chlorogenic acid (isomer: Neochlorogenic acid)	354.3		++	+	++++	++++
7 Afzelin	432.38		-	+	-	+
8 Quercitrin (isomer: Quercetin 3-O-alpha-rhamnoside)	448.38		++	++++	+++	+++
9 Hyperoside (isomer: Hyperin, Isoquercitrin, quercetin-3-O-galactoside)	464.38		+	++	++	++
10 Rutin	610.5		-	-	+	+

*Phenolic acids: (1) 4-Vinylcatechol, (2) Caffeic acid, (4) Ferulic acid, (6) Chlorogenic acid (isomer: Neochlorogenic acid).

*flavonoids: (5) Quercetin, (7) afzelin, (8) Quercitrin (isomer: Quercetin 3-O- α -rhamnoside), (9) Hyperoside (isomer: Hyperin, Isoquercitrin/quercetin-3-O-galactoside), (10) Rutin.

*non-phenolic substances: (3) Quinic acid.

*note.

<-> defined as signal of relative abundance is lower than 5.

<+> defined as signal of relative abundance is lower than 25 and bigger than 5.

<+++> defined as signal of relative abundance is lower than 50 and bigger than 25 <++++> defined as signal of relative abundance is lower than 75 and bigger than 50.

<++++> defined as signal of relative abundance is higher than 75.

ES-like structural features are encircled.

On the other hand, for the pure water extraction, the extract after cyclic voltammetry scanning is greater than the unscanned extract, and the EC₅₀ ranking as follows: water extract before CV \approx water extract after CV (Table 5). These all suggested that CV treatment could be a novel alternative to process herbal medicine to be less toxic and more efficacious for disease treatment.

Moreover, Table 5 also clearly exhibited that CV treatment upon 60% ethanol extract could increase antioxidant activity ca. $10^{6.452-3.907} \approx 350$ -fold, clearly present the promising feasibility to use such a method to process *H. cordata* extract. The effect of water polarity on ethanol and contributing effect to the antioxidant capacity can be observed by comparing the pure water and ethanol extracts. The relative position of the dose-response curve was used to assess the DPPH radical scavenging ability of the two extracts (Fig. 6). Since the results of the previous analysis (Table 3) are very close to 50–70% ethanol extraction results, the concentration of the mid value was selected. The ranking of EC₅₀ also showed: 60% ethanol extraction > 0% water extraction; thus, the 60% ethanol extraction was chosen for relative comparison. From Fig. 6, the 60% ethanol extract arises as the significant curve on the upper left side of the figure suggests a higher scavenging activity (Fig. 6). Compared with the 60% stock solution, EC₅₀ is increased, but the EC₅₀ of the water extraction had a slight change in DPPH, similar to prior results in TPC. The scavenging rate of the 60% ethanol extract after CV is much higher than that of the water extract. The results also suggest that the presence of water is helpful for the extraction of polyphenols [49]. It can thus be suggested that the polyphenol content was indeed directly related to the free radical scavenging activity.

3.5. Analysis of LC-MS/MS Results

3.5.1. Fundamental analysis

Ethanol, a polar solvent, can efficiently extract flavonoids (e.g., their glycosides, catechols, and tannins) from raw herbal materials. Extraction efficiency can be further enhanced by mixing solvents to further improve the solubility of these compounds for a limited range of components [50]. Some chemicals with electrochemical functional groups (e.g., -OH and -NH substituents) can act as electron shuttles through the proposed interconversion pathway. As a result of the acidic nature of the hydroxyl group (-OH) of phenols, acidic hydrogen can be abstracted to obtain phenate anions which will then be efficiently oxidized to form active radicals [51]. These radical formation steps are key in triggering redox mediators to stimulate the electron transfer and bioelectricity generation.

Chemical composition of *H. cordata* contains abundant polyphenols, fatty acids, flavonoids, and alkaloids. LC/MS result analysis chart is used to distinguish the differences in the substances contained in the extract. Through Electrospray Ionization (ESI) atomization, the sample will generate positively or negatively charged ions and the analysis in this study was completed in a negative ion environment (Figs. 11 and 12) [9–11,43] (Table 6). The peaks marked with Arabic numerals on the graph represent different components and the strength of the signal is based on the amount of "+."

3.5.2. The effect of structural formula on redox ability

Both polyphenolics and flavonoids in herbal extracts are often

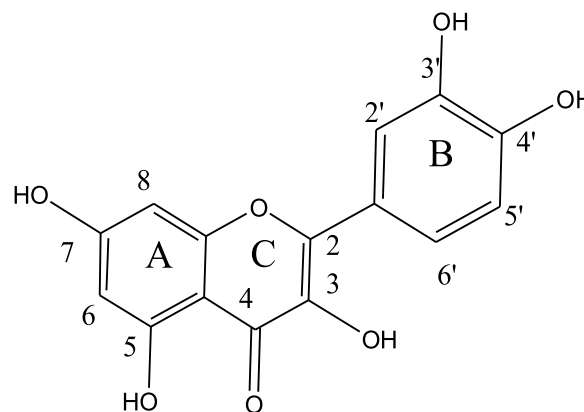


Fig. 7. The Structural formula of flavonoid.

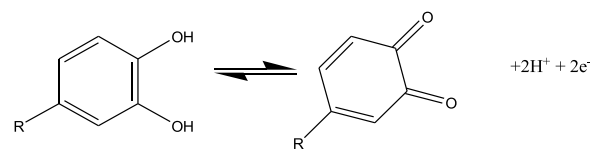


Fig. 8. This form is the process of the redox reaction of phenolic acids.

considered to possess good electrochemical properties. According to literature, dihydroxyl substituents-bearing chemicals manifesting ES-related structures can become *ortho*- and *ortho*-phthalquinones after continuous CV scanning [21,52]. The electrochemical properties of flavonoids, similar to their redox behavior, are mainly driven by the stability of the phenoxyl radicals through electricity generation. As a matter of fact, these all are associated to electron-transporting capabilities. The ability of electron transfer is also a keystone parameter to influence the capability of antioxidants to reduce oxidants. Therefore, the structural relationship is of great importance, especially the number and relative position of the hydroxyl substituents on the aromatic ring. The electrical activity is related to the A and B ring and phenolic group, which directly determines the electrochemical properties. Choosing quercetin as an example, catechol is present in the B ring (Fig. 7). For the catechol group, studies have shown that quercetin produces 3 oxidation peaks after cyclic voltammetry, meaning that there are three places where quinones will form. However, there is only one reduction peak thus only 2 peaks are leading to oxidation where there are only two places where quinones will form. Hence, such structures would not be stable, resulting in the presence of lone electrons that generate active free radicals [37,38].

At electrochemically favorable conditions, phenolic acids and flavonoids could be oxidized to form quinones due to the modifications in their structures. Many studies mentioned such substances as antioxidants (e.g., phenolic acids and flavonoids). However, their nature of electrochemical reversibility of ESs was rare to be disclosed. In fact, the transformation of oxidants in the structure is by releasing/binding electrons/protons to form quinones, and then successive oxidation and/or reduction reversibly was taken place toward to their original state

(Fig. 8). Using quercetin as an example, due to the electron-withdrawing effect of the C ring, the nucleophile leads to the oxidation of -OH on the A ring. That is, this oxidation occurs at a higher potential, and the presence of water and/or ethanol in the solution (i.e., specific electrochemical conditions) significantly affects the oxidation mechanism and antioxidant activity [47]. Water can act as a catalyst in the reaction due to the formation of quinone in the ortho-position [37,53]. The proper combination of protonation and reduction sequence of polyphenols may be the key mechanism to control the action of polyphenolic antioxidants as ES. As the literature indicated, at the appropriate pH value, more phenols may be unstable oxidation or reduction, which can result not only in the increase of the antioxidant activity but also in the increase of ES capability [24]. That is, environmental manipulation directly affects the characteristics of electrochemical reversibility of ESs and/or irreversibility of antioxidants.

The antioxidant or anti-radical activity is inversely proportional to its oxidation potential and the process of the redox reaction of phenolic acids (Table 6). According to Teixeira et al. [54], two phenols (e.g., caffeic acid, chlorogenic acid, and catechin alkaloid derivatives) showed high free radical scavenging activity and low oxidation potential. Individual phenols are less reactive and have higher reaction potentials but less than those of methoxy-substituted (e.g., ferulic acid). The electrochemical potential values depend on the redox behavior of the compounds, reflecting their ability to lose electrons. In general, the cyclic voltammetric results of phenolic acid derivatives will be similar to those observed for the mother compound [55].

As shown in Table 6, the proposed phenolic acids are mostly reduced after serial cyclic voltammetry scans. As Makhotkina and Kilmartin [38] pointed out, the redox characteristics would be achieved through the transfer of electrons (e.g., radical and adsorption). After cyclic voltammetry, the phenolic acids had indeed become *o*-phthalquinone. Since there is no excess hydroxyl group to cut them off, resulting in polymer formation. This polymer will form a thin film on the carbon shock (such that the electrode needs to be polished), possibly causing the area of the CV cycle (or electrochemical potential) to become gradually smaller. Most studies have shown that electron transfer processes of flavonoids are reversible and rarely irreversible [56,57]. According to studies, flavonoids would also decrease but from the previous analysis, the flavonoids increased and the substances in the mixed solution reacted with each other [52,58]. Some related chemical reactions cannot be directly and wholly expressed and can only be speculated. The extracts with flavonoid glycosides will promote the production of more flavonoids after CV scanning [47]. This speculation is based on the fact that the potential generated after CV scanning occurs at a larger value. The appearance of glycosylated flavonoids in the form of natural flavonoids makes these structures more stable and less prone to change [59]. These all reflected that whether the nature of flavonoids is either ESs or antioxidants would be strongly associated to the environment to be present.

3.5.3. Substance differences before and after CV

Introduction of polyphenolic-rich samples provided higher electricity production because of additional exogenous electron shuttles. Also, *Shewanella* has effectively utilized the converted nutrient sources because resulting nutrients in the medium have fewer carbon atoms, which is a conducive environment for strictly anaerobic microorganisms. This was supported after observing an increase percent ratio in the ethanol-water larger than water extract from the before CV to after CV. This suggests that new substance(s) were formed to provide electrochemically favorable stimulation to bioelectricity generation of *Shewanella*. After the substances in the water extract were subjected to CV, the low molecular weight substances were significantly reduced wherein quinic acid was the most reduced. However, aware that quinic acid is not a phenolic acid. It is presented as relative content; hence, it will be compared with substances with relatively large content. Flavonoids and their glycosides are very stable in the extract. Previously, the water extract was tested using the electric power density. After CV, it also

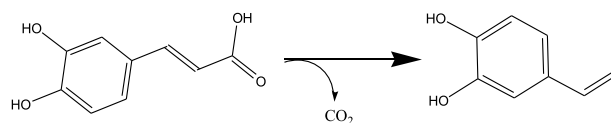


Fig. 9. Decarboxylation of caffeic acid to produce highly reactive 4-vinylcatechol.

increased by 30% compared with before CV and it was also confirmed that glycosides stably existed [60]. Through the scanning of different CV cycles from previous studies, the potential of flavonoid glycosides is higher than that of flavonoids and phenolic acids [38,55,61,62]. The second oxidation peak of water extraction appeared at a higher potential, but the changes were minimal. It can be understood that this oxidation peak may be glycoside but the amount that appeared after the CV scan was not noticeable. That is, the formed oxidation peak is less significant. It is known from the literature that the phenolic acids (Table 6), will indeed become *o*-phthalquinones after cyclic voltammetry. It has been previously shown that the continuous oxidation of phenolic acids resulting in the formation of polymers on the glassy carbon electrode is an irreversible phenomenon [38,56]. This result indicated that phenolic acids are not electrochemically suitable as ES. In contrast, not all antioxidants can be used as ES and only chemical substances that can be completely retained in the solution can be used as ES [38,63].

After the substances in the ethanol extraction had undergone CV, from the results of the quinic acid and phenolic acids in the ethanol and water extracts, the signal attenuation was smaller, and the substances contained before and after CV significantly changed. However, it is not large and is found in CV profiles of ethanol extracts. Notably, there are two oxidation peaks in the first 10 cycles, where the oxidation peak gradually disappears in the 10~50 cycles, and finally, the second oxidation peak appears again in the 50~100 cycles. However, this also means that the composition of the polyphenols in the mixture was chemically transformed. Although the signal of phenolic acids minutely changed, it was presumed that more flavonoids and glycosides appeared after CV. This presumption is known from the CV figure, where the potential of flavonoid glycosides will be higher than that of flavonoids and phenolic acids, and the potential of the second oxidation peak is indeed gradually attenuating [38,61]. Flavonoids have been confirmed in several studies as good ESs and a recent study showed that the presence of flavonoid glycosides can accelerate the oxidation of phenolic substances to form quinones which can generate nucleophilic resonance through chemical structures [5,20,38,47]. Quinones formed via

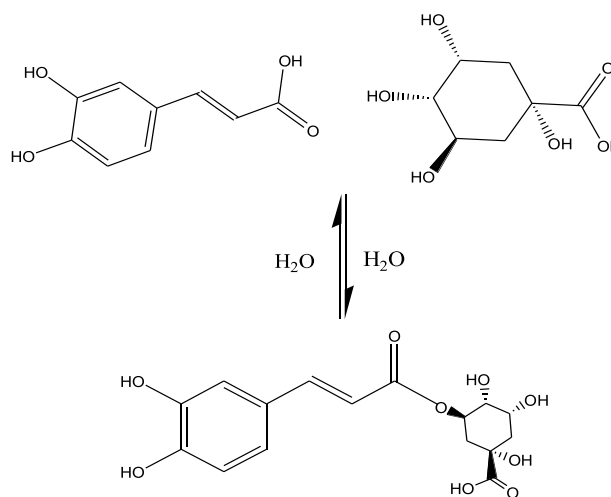


Fig. 10. Esterification of caffeic acid and quinic acid to produce chlorogenic acid.

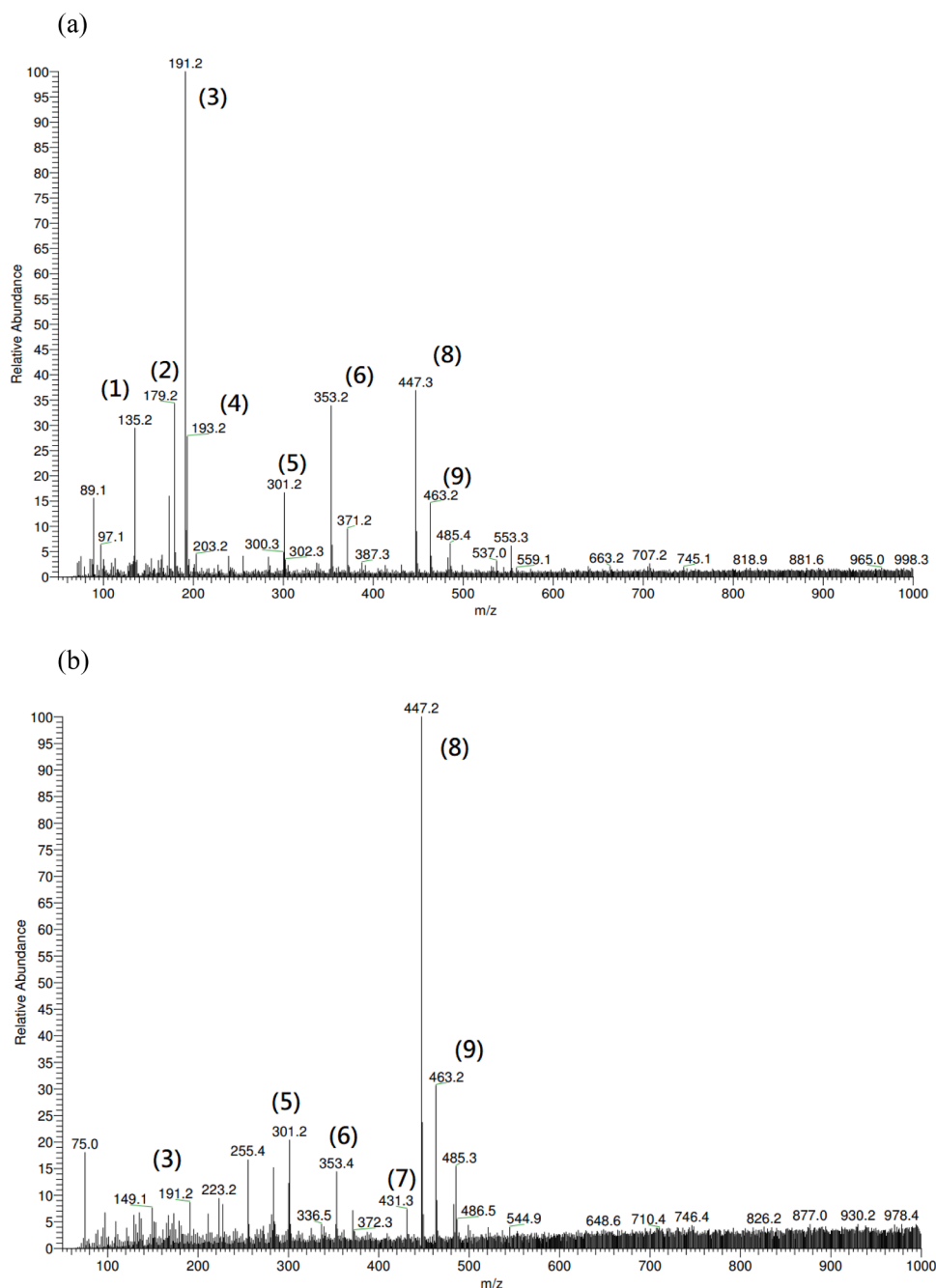


Fig. 11. LC/MS chromatogram of *H. cordata* pure water extract (a) Without CV scan, (b) After 100 cycles of CV scan, * Molecular weights indicated by numbers refer to Table 6.

flavonoids oxidation can be effectively reduced [58]. The increase of flavonoids and glycosides in the extracts after CV resulted in an increase in the bioactivity of *H. cordata* extract and a decrease in the inhibitory substances. In the analysis of electric power density, the extract after CV scanning as an additive was higher than before CV scanning. It is reasonable to infer that most of the increased polyphenols are very likely flavonoids and their glycosides [60].

In plants, caffeic acid can be covalently linked to cell wall polysaccharides and exists mainly with quinic acid or esterified forms of glucose such as chlorogenic acid (5-O-caffeoylquinic acid) and its isomers. While chlorogenic acid can be present in various forms, depending on the position of the ester bond, several isomeric forms will be found such as neochlorogenic acid (3-O-caffeoylquinic acid) and cryptochlorogenic acid (4-O-caffeoylquinic acid) [11,64]. The esterification of

caffeic acid and quinic acid to produce chlorogenic acid will release caffeic acid through hydrolysis and caffeic acid will produce highly reactive 4-vinyl catechol after decarboxylation (Fig. 9). The simultaneous thermal elimination of the acid may directly yield 4-vinylcatechol, and the caffeic acid may also undergo hydroxylation to form chlorogenic acid (Fig. 10) [19,38].

3.5.4. The difference between water extraction and ethanol extraction

Most of aforementioned results indicated that ethanol extract exhibited higher antioxidant activity and polyphenol content. Nevertheless, the AUC of the water extract was larger, according to the CV results. It was previously indicated that the polymer formed by the redox of phenolic acids possibly caused the clogging of the glassy carbon electrode [37,38]. Therefore, the amount of polymer likely indicates the

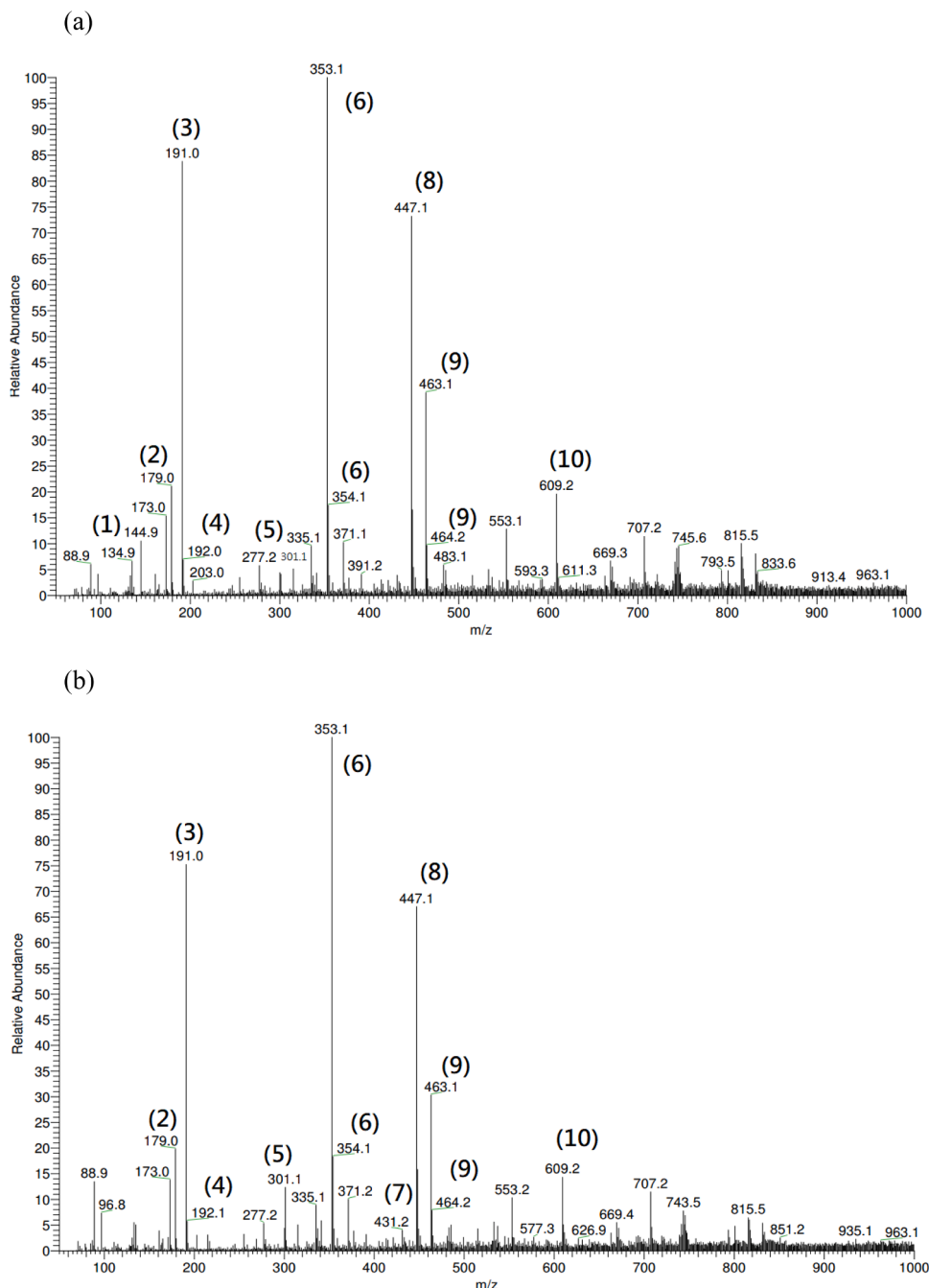


Fig. 12. LC/MS chromatogram of *H. cordata* 60% ethanol extract (a) Without CV scan, (b) After 100 cycles of CV scan, * Molecular weights indicated by numbers refer to Table 6.

clogging degree of phenolic acids. Specifically, the larger the AUC, the lower the clogging degree. This results in the total polyphenol content in ethanol extract higher than that in water extract.

The content of rutin is only found in the ethanol extract. It is incompatible with water. According to Peng et al. [65], it can be seen that the solubility of rutin in pure water and ethanol aqueous solution varies as the crystal structure changes. According to the study, rutin will undergo two oxidations and one reduction. The first oxidation will form quinone and there will be a corresponding reduction peak. This reaction will be reversible. In the second oxidation, the reaction occurred at a higher potential, and no corresponding reduction peak appeared, indicating the electrochemical irreversibility of oxidation process. Overall, the quinone species will be reduced due to the reversibility of the first oxidation which fully shows that the rutin undergoes reduction after CV

[58].

CV and MFC analysis results differed from those of TPC, DPPH, and PD. There are several possible reasons for the inconsistency between the results of CV and PD, TPC, and DPPH as follows: (1) Not all substances that can undergo redox are antioxidants and the antioxidant properties of the substances need to be understood by using the level of oxidation potential; (2) The quinone formed by oxidation cannot be restored smoothly, hence the reduction peak decreases over repeated exposure; and (3) *H. cordata* extract may have biotoxicity potency on electroactive bacteria; thereby, affecting the bioelectricity characteristics in MFCs to be repressed. As LC/MS results indicated, the flavonoid glycosides of *H. cordata* extract increased after CV treatment; hence, its antioxidant activity also increased as shown in Table 6, Fig. 11, and Fig. 12 [62]. Moreover, electrochemical activity was also found to increase. It is

Table 7

Binding affinity of quercitrin compared with the positive controls.

Protein code	Binding Energy (kcal/mol)		Reference(s)
	Quercitrin	Control	
7BTF*	-6.6	-6.1	(Remdesivir) [68,69]
1R42	-1.4	-4.6	(MLN-4760) [70,71]

^aQuercitrin was observed to have promising binding affinity on this protein.

possible to hypothesize that the intermediates and derived products of electrochemical conversion can still effectively express redox activity and be used as ESs. Consequently, it is also found that CV scanning can effectively reduce toxicity potency or increase the electrochemical activity of *H. cordata* extracts. Lastly, the findings suggest that flavonoid glycosides are good antioxidants and also a class of ES.

3.6. Molecular docking Studies

3.6.1. Molecular docking analysis

For the structural validation of the processed protein, all six proteins

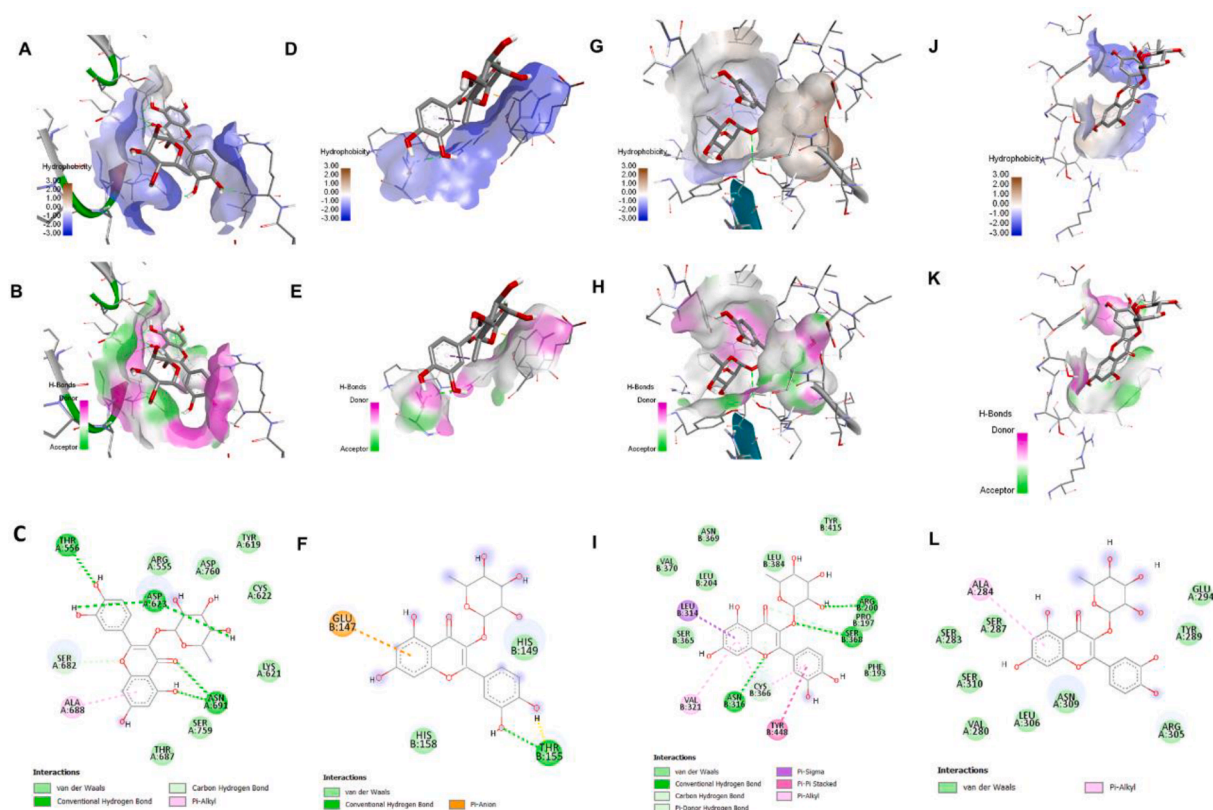


Fig. 13. Binding interaction of quercitrin and the proteins (SARS-CoV-2 RdRp): Hydrophobic (A, D, G, J) and H-bond property (B, E, H, K) of binding pocket, 2-D.

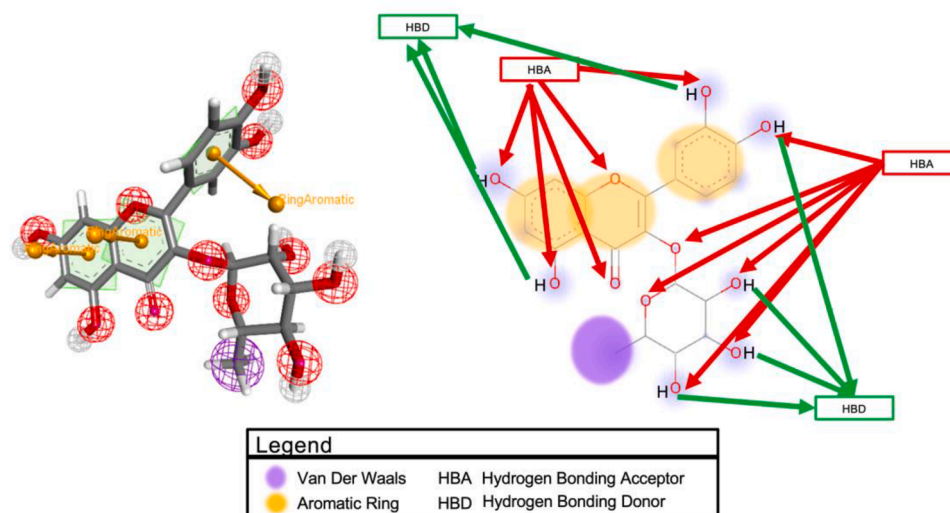


Fig. 14. Pharmacophore descriptor of quercitrin.

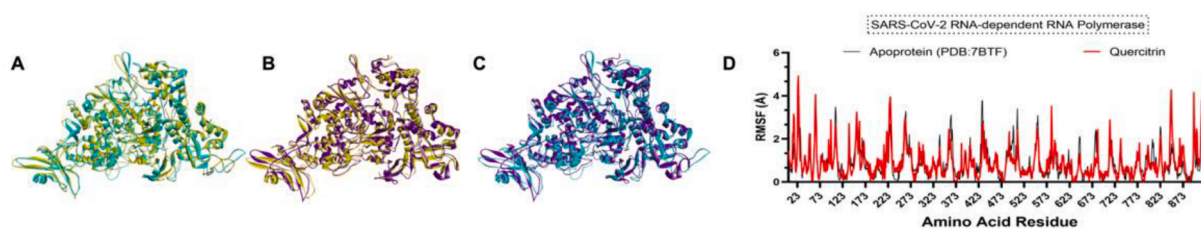


Fig. 15. Molecular Dynamics Simulation of Protein-Quercitrin complexes: SARS-CoV-2 RdRp (A-D).

Table 8

Average RMSF value of the bounded and unbounded protein.

Protein	Average RMSF (Å)	
Apoprotein	Bounded with ligand	
SARS-CoV-2 RdRp	0.8862±0.024	0.9070±0.024

meet the criteria set for each algorithm used for protein model validation. Among all proteins, quercitrin does exhibit a promising binding affinity (as compared to the control against SARS-CoV-2 RdRp (7BTF) and ACE-2 receptor (1R42) (Table 7). The properties (e.g., hydrophobic and hydrophilic) of the binding pocket and amino acid residues interacting with the ligand are shown in Fig. 13. Other than van der Waals forces, hydrogen bonding was the predominating non-bonding interaction observed in the ligand association. By looking at the pharmacophore descriptor of the ligand, it was not surprising to have such an observation (Fig. 14). The hydroxyl group present in the quercitrin is readily available to act as a hydrogen bonding acceptor or donor during interaction [66]. Other than hydrogen bonding, aromatic rings of the quercitrin do also participate in protein-ligand interaction by Pi-Alkyl, Pi-Anion, Pi-Sigma, Pi donor hydrogen bond, Pi-Pi Stacked [67]. Carbon-hydrogen bonding (from aromatic to amino acid residues) was also observed during the binding of quercitrin to SARS-CoV-2 RdRp. Protein-ligand complexes with promising binding energy were subjected to molecular dynamics simulation to further study the possible changes in the protein conformational and flexibility.

3.6.2. Molecular dynamics analysis

A 10 ns molecular dynamics simulation was performed with the complexes and the results are shown in Fig. 15. The changes of the apoprotein (Initial:Yellow; 10 ns: Sky Blue) and bounded protein (Initial: Yellow, 10 ns: Violet) were compared in Fig. 15C (SARS-CoV-2 RdRp). The result is the average RMSF value of bounded and unbounded proteins (Table 8). Upon binding of quercitrin, the dengue viral entry protein became stiffer as compared to the apoprotein. While the other three proteins became more flexible than the apoprotein. Such observation may be caused by the conformation of the ligand for protein binding that can affect the types of non-bonding interaction participating in the action [72]. Overall, the changes in the flexibility of the bounded were insignificant by looking at the RMSF graph and t-test (using GraphPad) analysis. Therefore, it is worth conducting further studies on quercitrin as a broad-range antiviral drug. Specifically, quercitrin is a glycoside derivative of flavonoids, and quercitrin shows a promising binding affinity over several viral proteins in this study. Such findings, therefore, support the connections of electron shuttling capability with antiviral activity. Binding of the SARS-CoV-2 spike protein to the angiotensin converting enzyme 2 (ACE2) promotes cellular entry. Its peptidase activity is critical for the virion to gain access into the host cytosol. Agricultural herbs with good bioelectricity-generating performance in MFCs have implicated great importance as potential anti-viral agents. This is because these compounds are “reversible catalysts” that effectively mediate in redox reactions that may provide persistent efficacy as antivirals once explored [12,73].

4. Conclusion

The leaves of *H. cordata* are analyzed and compared using CV, TPC, DPPH, and MFCs. The results of the electricity production evaluation showed that the extract of the leaves is indeed a potential source of electron shuttles. The results of TPC, DPPH, and PD are consistent, wherein the results of TPC and DPPH indicate that polyphenols from *H. cordata* extracts are also key substances with electron-shuttling potential. However, consequent CV analysis reveals that flavonoid substances were more electrochemically stable after continuous redox reactions. Therefore, this study concluded that flavonoids would exhibit more promising electron shuttling characteristics than polyphenols. From the LC/MS and structural analysis of CV scanned extracts, the oxidation potential of flavonoid glycosides was greater than that of flavonoids and phenolic acids as a result of the changes in the extract. To compare solvent extraction, 60% ethanol extracts exhibited the highest flavonoid content, which was also revealed to increase the efficiency of bioelectricity generation. Lastly, molecular docking analysis reveals quercetin as a potential antiviral drug for COVID-19 and a foundational link between antiviral with electron shuttling capability.

CRedit authorship contribution statement

Chia-Kai Lin: Conceptualization, Data curation, Formal analysis, Funding acquisition, Investigation, Methodology, Visualization, Writing – original draft. **Bor-Yann Chen:** Data curation, Formal analysis, Writing – review & editing. **Jasmine U. Ting:** Data curation, Formal analysis, Writing – review & editing. **Kristian Gil G. Rogio:** Data curation, Formal analysis, Writing – review & editing. **Po-Wei Tsai:** Data curation, Formal analysis, Investigation, Supervision, Validation, Visualization, Writing – original draft, Writing – review & editing. **Yung-Chuan Liu:** Conceptualization, Data curation, Formal analysis, Funding acquisition, Investigation, Methodology, Visualization, Writing – original draft, Supervision, Validation, Writing – review & editing.

Declaration of Competing Interest

The authors declare that they have no known competing financial interests or personal relationships that could have appeared to influence the work reported in this paper.

Acknowledgments

The authors sincerely appreciate financial supports from the Taiwan's Ministry of Science and Technology. This work was also partially supported by Taiwan's Ministry of Education (108-109 TEEP@AsiaPlus Program) and Taiwan's Ministry of Science and Technology (MOST-109-2622-E-005 -002 -CC3 and MOST 109-2221-E-197-016-MY3).

References

- [1] Tian L, Zhao Y, Guo C, Yang X. A comparative study on the antioxidant activities of an acidic polysaccharide and various solvent extracts derived from herbal *Houttuynia cordata*. *Carbohydr Polym* 2011;83:537–44. <https://doi.org/10.1016/j.carbpol.2010.08.023>.

- [2] Luo L, Jiang J, Wang C, Fitzgerald M, Hu W, Zhou Y, Zhang H, Chen S. Analysis on herbal medicines utilized for treatment of COVID-19. *Acta Pharm Sin B* 2020;10:1192–204. <https://doi.org/10.1016/j.apsb.2020.05.007>.
- [3] Chioh KH, Phoon MC, Putti T, Tan BKH, Chow VT. Evaluation of antiviral activities of *Houttuynia cordata* thunb. extract, quercetin, quercetrin and cinanserin on murine coronavirus and dengue virus infection. *Asian Pac J Trop Med* 2016;9:1–7. <https://doi.org/10.1016/j.apjtm.2015.12.002>.
- [4] Yuan H, Liu L, Zhou J, Zhang T, Daily JW, Park S. Bioactive components of *Houttuynia cordata* thunb and their potential mechanisms against COVID-19 using network pharmacology and molecular docking approaches. *J Med Food* 2022;25:355–66. <https://doi.org/10.1089/jmf.2021.K.0144>.
- [5] Tsai PW, Hsueh CC, Yang HC, Tsai HY, Chen BY. Interactive deciphering electron-shuttling characteristics of agricultural wastes with potential bioenergy-steered anti-COVID-19 activity via microbial fuel cells. *J Taiwan Inst Chem Eng* 2022;136:104426. <https://doi.org/10.1016/j.jtice.2022.104426>.
- [6] Huang ZL, Chen BY, Liu YC. Optimal stimulation of *Houttuynia cordata* herbal extract as electron shuttle for bioenergy extraction in microbial fuel cells. *J Taiwan Inst Chem Eng* 2020;114:47–56. <https://doi.org/10.1016/j.jtice.2020.09.026>.
- [7] Shingnaisui K, Dey T, Manna P, Kalita J. Therapeutic potentials of *Houttuynia cordata* thunb. against inflammation and oxidative stress: a review. *J Ethnopharmacol* 2018;220:35–43. <https://doi.org/10.1016/j.jep.2018.03.038>.
- [8] Lau KM, Lee KM, Koon CM, Cheung CSF, Lau CP, Ho HM, Lee MYH, Au SWN, Cheng CHK, Lau CBS, Tsui SKW, Wan DCC, Waye MMY, Wong KB, Wong CK, Lam CWK, Leung PC, Fung KP. Immunomodulatory and anti-SARS activities of *Houttuynia cordata*. *J Ethnopharmacol* 2008;118:79–85. <https://doi.org/10.1016/j.jep.2008.03.018>.
- [9] Yang ZN, Sun YM, Luo SQ, Chen JW, Chen JW, Yu ZW, et al. Quality evaluation of *Houttuynia cordata* Thunb. by high performance liquid chromatography with photodiode array detection (HPLC-DAD). *Pak J Pharm Sci* 2014;27:223–31.
- [10] Meng J, Leung KSY, Jiang Z, Dong X, Zhao Z, Xu LJ. Establishment of HPLC-DAD-MS fingerprint of fresh *Houttuynia cordata*. *Chem Pharm Bull* 2005;53:1604–9. <https://doi.org/10.1248/cpb.53.1604>. Tokyo.
- [11] Nuengchamnong N, Krittasilp K, Ingkaninan K. Rapid screening and identification of antioxidants in aqueous extracts of *Houttuynia cordata* using LC–ESI–MS coupled with DPPH assay. *Food Chem* 2009;117:750–6. <https://doi.org/10.1016/j.foodchem.2009.04.071>.
- [12] Sun W, Lin Z, Yu Q, Cheng S, Gao H. Promoting extracellular electron transfer of *Shewanella oneidensis* MR-1 by optimizing the periplasmic cytochrome C network. *Front Microbiol* 2021;12. <https://doi.org/10.3389/fmicb.2021.727709>.
- [13] Slate AJ, Whitehead KA, Brownson DAC, Banks CE. Microbial fuel cells: an overview of current technology. *Renew Sustain Energy Rev* 2019;101:60–81. <https://doi.org/10.1016/j.rser.2018.09.044>.
- [14] Abbassi R, Yadav AK. Introduction to microbial fuel cells: challenges and opportunities. integrated microbial fuel cells for wastewater treatment. Elsevier 2020:3–27. <https://doi.org/10.1016/B978-0-12-817493-7.00001-1>.
- [15] Chen BY, Hsueh CC, Liu SQ, Hung JY, Qiao Y, Yueh PL, Wang YM. Unveiling characteristics of dye-bearing microbial fuel cells for energy and materials recycling: redox mediators. *Int J Hydrog Energy* 2013;38:15598–605. <https://doi.org/10.1016/j.ijhydene.2013.03.132>.
- [16] Xu B, Chen BY, Hsueh CC, Qin LJ, Chang CT. Deciphering characteristics of bicyclic aromatics – mediators for reductive decolorization and bioelectricity generation. *Bioresour Technol* 2014;163:280–6. <https://doi.org/10.1016/j.biortech.2014.04.031>.
- [17] Chen BY, Ma CM, Liao JH, Hsu AW, Tsai PW, Wu CC, Hsueh CC. Feasibility study on biostimulation of electron transfer characteristics by edible herbs-extracts. *J Taiwan Inst Chem Eng* 2017;79:125–33. <https://doi.org/10.1016/j.jtice.2017.04.024>.
- [18] Chen BY, Liao JH, Hsu AW, Tsai PW, Hsueh CC. Exploring optimal supplement strategy of medicinal herbs and tea extracts for bioelectricity generation in microbial fuel cells. *Bioresour Technol* 2018;256:95–101. <https://doi.org/10.1016/j.biortech.2018.01.152>.
- [19] Hsueh CC, Wu CC, Chen BY. Polyphenolic compounds as electron shuttles for sustainable energy utilization. *Biotechnol Biofuels* 2019;12:271. <https://doi.org/10.1186/s13068-019-1602-9>.
- [20] Zhang S, Qu Z, Hsueh CC, Chang CT, Chen BY. Deciphering electron-shuttling characteristics of *Scutellaria baicalensis* Georgi and ingredients for bioelectricity generation in microbial fuel cells. *J Taiwan Inst Chem Eng* 2019;96:361–73. <https://doi.org/10.1016/j.jtice.2018.12.001>.
- [21] Guo LL, Qin LJ, Xu B, Wang XZ, Hsueh CC, Chen BY. Deciphering electron-shuttling characteristics of epinephrine and dopamine for bioenergy extraction using microbial fuel cells. *Biochem Eng J* 2019;148:57–64. <https://doi.org/10.1016/j.bej.2019.04.018>.
- [22] Tsai PW, Hsieh CY, Ting JU, Rogio KGG, Lee CJ, De Castro-Cruz KA, Ciou YR, Lien TK, Yang LL, Hsueh CC, Chen BY. Unraveling the bioenergy production and electron transport characteristics of processed *Rheum palmatum* L. for antiviral drug development. *Ind Crops Prod* 2023;195:116488. <https://doi.org/10.1016/j.indcrop.2023.116488>.
- [23] Tsai PW, Tayo LL, Ting JU, Hsieh CY, Lee CJ, Chen CL, Yang HC, Tsai HY, Hsueh CC, Chen BY. Interactive deciphering electron-shuttling characteristics of *Coffea arabica* leaves and potential bioenergy-steered anti-SARS-CoV-2 RdRp inhibitor via microbial fuel cells. *Ind Crops Prod* 2023;191:115944. <https://doi.org/10.1016/j.indcrop.2022.115944>.
- [24] Chen BY, Liao JH, Hsueh CC, Qu Z, Hsu AW, Chang CT, Zhang SP. Deciphering biostimulation strategy of using medicinal herbs and tea extracts for bioelectricity generation in microbial fuel cells. *Energy* 2018;161:1042–54. <https://doi.org/10.1016/j.energy.2018.07.177>.
- [25] Pudziulyte L, Jakštas V, Ivanauskas L, Laukevičienė A, Ibe CFD, Kursvietienė L, Bernatoniene J. Different extraction methods for phenolic and volatile compounds recovery from *Elsholtzia ciliata* fresh and dried herbal materials. *Ind Crops Prod* 2018;120:286–94. <https://doi.org/10.1016/j.indcrop.2018.04.069>.
- [26] Chevon S, Roberts MA, Chevon M. The use of cyclic voltammetry for the evaluation of antioxidant capacity. *Free Radic Biol Med* 2000;28:860–70. [https://doi.org/10.1016/S0891-5849\(00\)00178-7](https://doi.org/10.1016/S0891-5849(00)00178-7).
- [27] Cassiana Frohlich P, Andressa Santos K, Din Mahmud Hasan S, Antônio da Silva E. Evaluation of the ethanolic ultrasound-assisted extraction from clove (*Syzygium aromaticum*) leaves and chemical characterization of the extracts. *Food Chem* 2022;373:131351. <https://doi.org/10.1016/j.foodchem.2021.131351>.
- [28] Oliveira GK, Tormin TF, Sousa RM, de Oliveira A, de Moraes SA, Richter EM, Munoz RA. Batch-injection analysis with amperometric detection of the DPPH radical for evaluation of antioxidant capacity. *Food Chem* 2016;192:691–7. <https://doi.org/10.1016/j.foodchem.2015.07.064>.
- [29] Janeiro P, Oliveira Brett AM. Catechin electrochemical oxidation mechanisms. *Anal Chim Acta* 2004;518:109–15. <https://doi.org/10.1016/j.aca.2004.05.038>.
- [30] Rizvi SMD, Shakil S, Haneef M. A simple click by click protocol to perform docking: autodesk 4.2 made easy for non-bioinformaticians. *EXCLI J* 2013;12:831–57.
- [31] Wallner B, Elofsson A. Identification of correct regions in protein models using structural, alignment, and consensus information. *Protein Sci* 2006;15:900–13. <https://doi.org/10.1110/ps.051799606>.
- [32] Dym O, Eisenberg D, Yeates TO. Detection of errors in protein models. International tables for crystallography. Chester, England: International Union of Crystallography; 2006. p. 520–30. <https://doi.org/10.1107/97809553602060000709>.
- [33] O'Boyle NM, Banck M, James CA, Morley C, Vandermeersch T, Hutchison GR. Open babel: an open chemical toolbox. *J Cheminform* 2011;3:33. <https://doi.org/10.1186/1758-2946-3-33>.
- [34] Schneidman-Duhovny D, Dror O, Inbar Y, Nussinov R, Wolfson HJ. PharmaGist: a webserver for ligand-based pharmacophore detection. *Nucleic Acids Res* 2008;36:W223–8. <https://doi.org/10.1093/nar/gkn187>.
- [35] Trott O, Olson AJ. AutoDock vina: improving the speed and accuracy of docking with a new scoring function, efficient optimization, and multithreading. *J Comput Chem* 2009. <https://doi.org/10.1002/jcc.21334>. NA-NA.
- [36] Kuriata A, Gierut AM, Oleniecki T, Ciemny MP, Kolinski A, Kurcinski M, Kmiecik S. CABS-flex 2.0: a web server for fast simulations of flexibility of protein structures. *Nucleic Acids Res* 2018;46:W338–43. <https://doi.org/10.1093/nar/gky356>.
- [37] Timbola AK, de SCD, Giacomelli C, Spinelli A. Electrochemical oxidation of quercetin in hydro-alcoholic solution. *J Braz Chem Soc* 2006;17:139–48. <https://doi.org/10.1590/S0103-50532006000100020>.
- [38] Makhotkina O, Kilmartin PA. The use of cyclic voltammetry for wine analysis: determination of polyphenols and free sulfur dioxide. *Anal Chim Acta* 2010;668:155–65. <https://doi.org/10.1016/j.aca.2010.03.064>.
- [39] Fu J, Dai L, Lin Z, Lu H. *Houttuynia cordata*; thunb: a review of phytochemistry and pharmacology and quality control. *Chin Med* 2013;04:101–23. <https://doi.org/10.4236/cm.2013.43015>.
- [40] Ju ZY, Howard LR. Effects of solvent and temperature on pressurized liquid extraction of anthocyanins and total phenolics from dried red grape skin. *J Agric Food Chem* 2003;51:5207–13. <https://doi.org/10.1021/jf0302106>.
- [41] Mokrani A, Madani K. Effect of solvent, time and temperature on the extraction of phenolic compounds and antioxidant capacity of peach (*Prunus persica* L.) fruit. *Sep Purif Technol* 2016;162:68–76. <https://doi.org/10.1016/j.seppur.2016.01.043>.
- [42] Tan MC, Tan CP, Ho CW. Effects of extraction solvent system, time and temperature on total phenolic content of henna (*Lawsonia inermis*) stems. *Int Food Res J* 2013;20:3117–23.
- [43] Chen BY, Lai YT, Hsueh CC. Synergic efficacy of bioenergy expression for compound herbal medicine of Parkinson's disease: The methods of replacement series and concentration addition. *J Taiwan Inst Chem Eng* 2022;137:104208. <https://doi.org/10.1016/j.jtice.2022.104208>.
- [44] Hsueh CC, Chen CT, Hsu AW, Wu CC, Chen BY. Comparative assessment of azo dyes and nitroaromatic compounds reduction using indigenous dye-decolorizing bacteria. *J Taiwan Inst Chem Eng* 2017;79:134–40. <https://doi.org/10.1016/j.jtice.2017.04.017>.
- [45] Han K, Yueh PL, Qin LJ, Hsueh CC, Chen BY. Deciphering synergistic characteristics of microbial fuel cell-assisted dye decolorization. *Bioresour Technol* 2015;196:746–51. <https://doi.org/10.1016/j.biortech.2015.08.015>.
- [46] Chen CC, Su YC. An autonomous CO₂ discharge and electrolyte agitation scheme for portable microbial fuel cells. *J Micromech Microeng* 2007;17:S265–73. <https://doi.org/10.1088/0960-1317/17/9/S09>.
- [47] Naróg D. Electrochemical study of quercetin in the presence of galactopyranose: potential application to the electrosynthesis of glycoconjugates of quinone/quinone methide of quercetin. *J Electroanal Chem* 2020;878:114675. <https://doi.org/10.1016/j.jelechem.2020.114675>.
- [48] Jeszka-Skowron M, Krawczyk M, Zgoła-Grzeżkowiak A. Determination of antioxidant activity, rutin, quercetin, phenolic acids and trace elements in tea infusions: Influence of citric acid addition on extraction of metals. *J Food Compos Anal* 2015;40:70–7. <https://doi.org/10.1016/j.jfca.2014.12.015>.
- [49] Li BB, Smith B, MdM H. Extraction of phenolics from citrus peels. *Sep Purif Technol* 2006;48:182–8. <https://doi.org/10.1016/j.seppur.2005.07.005>.
- [50] Spigno G, Tramelli L, De Faveri DM. Effects of extraction time, temperature and solvent on concentration and antioxidant activity of grape marc phenolics. *J Food Eng* 2007;81:200–8. <https://doi.org/10.1016/j.jfoodeng.2006.10.021>.

- [51] Chen BY, Wang YM, Ng IS, Liu SQ, Hung JY. Deciphering simultaneous bioelectricity generation and dye decolorization using *Proteus hauseri*. *J Biosci Bioeng* 2012;113:502–7. <https://doi.org/10.1016/j.jbiosc.2011.11.013>.
- [52] Gil ES, Couto RO. Flavonoid electrochemistry: a review on the electroanalytical applications. *Rev Bras Farmacogn* 2013;23:542–58. <https://doi.org/10.1590/S0102-695X2013005000031>.
- [53] Awad HM, Boersma MG, Boeren S, van Bladeren PJ, Vervoort J, Rietjens I. Structure–activity study on the quinone/quinone methide chemistry of flavonoids. *Chem Res Toxicol* 2001;14:398–408. <https://doi.org/10.1021/tx000216e>.
- [54] Teixeira J, Gaspar A, Garrido EM, Garrido J, Borges F. Hydroxycinnamic acid antioxidants: an electrochemical overview. *Biomed Res Int* 2013;2013:1–11. <https://doi.org/10.1155/2013/251754>.
- [55] Zielinska D, Wiczowski W, Piskula MK. Determination of the relative contribution of quercetin and its glucosides to the antioxidant capacity of onion by cyclic voltammetry and spectrophotometric methods. *J Agric Food Chem* 2008;56:3524–31. <https://doi.org/10.1021/jf073521f>.
- [56] Ghica ME, Brett A. Electrochemical oxidation of rutin. *Electroanalysis* 2005;17:313–8. <https://doi.org/10.1002/elan.200403100>.
- [57] Brett AMO, Ghica ME. Electrochemical oxidation of quercetin. *Electroanalysis* 2003;15:1745–50. <https://doi.org/10.1002/elan.200302800>.
- [58] He JB, Wang Y, Deng N, Zha ZG, Lin XQ. Cyclic voltammograms obtained from the optical signals: study of the successive electro-oxidations of rutin. *Electrochim Acta* 2007;52:6665–72. <https://doi.org/10.1016/j.electacta.2007.04.075>.
- [59] Plaza M, Pozzo T, Liu J, Gulshan Ara KZ, Turner C, Nordberg Karlsson E. Substituent effects on *in vitro* antioxidizing properties, stability, and solubility in flavonoids. *J Agric Food Chem* 2014;62:3321–33. <https://doi.org/10.1021/jf405570u>.
- [60] Benaiges-Fernandez R, Palau J, Offeddu FG, Cama J, Urmeneta J, Soler JM, Dold B. Dissimilatory bioreduction of iron(III) oxides by *Shewanella loihica* under marine sediment conditions. *Mar Environ Res* 2019;151:104782. <https://doi.org/10.1016/j.marenvres.2019.104782>.
- [61] Firuzi O, Lacanna A, Petrucci R, Marroso G, Saso L. Evaluation of the antioxidant activity of flavonoids by “ferric reducing antioxidant power” assay and cyclic voltammetry. *Biochim Biophys Acta (BBA) Gen Subj* 2005;1721:174–84. <https://doi.org/10.1016/j.bbagen.2004.11.001>.
- [62] Yamazaki E, Inagaki M, Kurita O, Inoue T. Antioxidant activity of Japanese pepper (*Zanthoxylum piperitum* DC.) fruit. *Food Chem* 2007;100:171–7. <https://doi.org/10.1016/j.foodchem.2005.09.036>.
- [63] Xie X, Chen Y, Bu Y, Dai C. A review of allelopathic researches on phenolic acids. *Acta Ecol Sin* 2014;34. <https://doi.org/10.5846/stxb201302210285>.
- [64] Cano-Marquina A, Tarín JJ, Cano A. The impact of coffee on health. *Maturitas* 2013;75:7–21. <https://doi.org/10.1016/j.maturitas.2013.02.002>.
- [65] Peng B, Li R, Yan W. Solubility of rutin in ethanol + water at (273.15 to 323.15) K. *J Chem Eng Data* 2009;54:1378–81. <https://doi.org/10.1021/je800816f>.
- [66] Raschka S, Wolf AJ, Bemister-Buffington J, Kuhn LA. Protein–ligand interfaces are polarized: discovery of a strong trend for intermolecular hydrogen bonds to favor donors on the protein side with implications for predicting and designing ligand complexes. *J Comput Aided Mol Des* 2018;32:511–28. <https://doi.org/10.1007/s10822-018-0105-2>.
- [67] Meyer EA, Castellano RK, Diederich F. Interactions with aromatic rings in chemical and biological recognition. *Angew Chem Int Ed* 2003;42:1210–50. <https://doi.org/10.1002/anie.200390319>.
- [68] Bravo JPK, Dangerfield TL, Taylor DW, Johnson KA. Remdesivir is a delayed translocation inhibitor of SARS-CoV-2 replication. *Mol Cell* 2021;81:1548–52. <https://doi.org/10.1016/j.molcel.2021.01.035>. e4.
- [69] Doharey PK, Singh V, Gedda MR, Sahoo AK, Varadwaj PK, Sharma B. *In silico* study indicates antimalarials as direct inhibitors of SARS-CoV-2-RNA dependent RNA polymerase. *J Biomol Struct Dyn* 2022;40:5588–605. <https://doi.org/10.1080/07391102.2021.1871956>.
- [70] Eweas AF, Alhossary AA, Abdel-Moneim AS. Molecular docking reveals ivermectin and remdesivir as potential repurposed drugs against SARS-CoV-2. *Front Microbiol* 2021;11. <https://doi.org/10.3389/fmicb.2020.592908>.
- [71] Towler P, Staker B, Prasad SG, Menon S, Tang J, Parsons T, Ryan D, Fisher M, Williams D, Dales NA, Patane MA, Pantoliano MW. ACE2 X-ray structures reveal a large hinge-bending motion important for inhibitor binding and catalysis. *J Biol Chem* 2004;279:17996–8007. <https://doi.org/10.1074/jbc.M311191200>.
- [72] Opo F, Rahman MM, Ahammad F, Ahmed I, Bhuiyan MA, Asiri AM. Structure based pharmacophore modeling, virtual screening, molecular docking and ADMET approaches for identification of natural anti-cancer agents targeting XIAP Protein. *Sci Rep* 2021;11:4049. <https://doi.org/10.1038/s41598-021-83626-x>.
- [73] Yaqoob AA, Mohamad Ibrahim MN, Rafatullah M, Chua YS, Ahmad A, Umar K. Recent advances in anodes for microbial fuel cells: an overview. *Materials* 2020;13:2078. <https://doi.org/10.3390/ma13092078>.